Naval Research Laboratory

Washington, DC 20375-5320

NRL/MR/6390--12-9380

Terahertz Spectra of Molecular Clusters of RDX, PETN, and TNT Calculated by Density Functional Theory

L. Huang
S.G. Lambrakos

Center for Computational Materials Science
Materials Science and Technology Division

A. Shabaev

George Mason University
Fairfax, Virginia

L. Massa

Hunter College
New York, New York

March 15, 2012

REPORT DOCUMENTATION PAGE

Form Approved
OMB No. 0704-0188

1. REPORT DATE *(DD-MM-YYYY)*	**2. REPORT TYPE**	**3. DATES COVERED** *(From - To)*
15-03-2012	NRL Memorandum Report	31-05-2010 – 30-11-2011

4. TITLE AND SUBTITLE

Terahertz Spectra of Molecular Clusters of RDX, PETN, and TNT Calculated by Density Functional Theory

5a. CONTRACT NUMBER

5b. GRANT NUMBER

5c. PROGRAM ELEMENT NUMBER

6. AUTHOR(S)

L. Huang, S.G. Lambrakos, A. Shabaev,* and L. Massa†

5d. PROJECT NUMBER

5e. TASK NUMBER

5f. WORK UNIT NUMBER
63-9465-02

7. PERFORMING ORGANIZATION NAME(S) AND ADDRESS(ES)

Naval Research Laboratory, Code 6394
4555 Overlook Avenue, SW
Washington, DC 20375-5320

8. PERFORMING ORGANIZATION REPORT NUMBER

NRL/MR/6390--12-9380

9. SPONSORING / MONITORING AGENCY NAME(S) AND ADDRESS(ES)

Office of Naval Research
One Liberty Center
875 North Randolph Street, Suite 1425
Arlington, VA 22203-1995

10. SPONSOR / MONITOR'S ACRONYM(S)
ONR

11. SPONSOR / MONITOR'S REPORT NUMBER(S)

12. DISTRIBUTION / AVAILABILITY STATEMENT

Approved for public release; distribution is unlimited.

13. SUPPLEMENTARY NOTES

*George Mason University, Department of Computation and Data Sciences, Fairfax, VA 22030
†Hunter College, City University of New York, New York, NY 10065

14. ABSTRACT

We present calculations of ground state resonance structure associated with molecular clusters of the high explosives RDX, PETN, and TNT using density functional theory (DFT), which is for the construction of parameterized dielectric response functions for excitation by electromagnetic waves at compatible frequencies. These dielectric functions provide for different types of analyses concerning the dielectric response of explosives. In particular, these dielectric response functions provide quantitative initial estimates of spectral response features for subsequent adjustment with respect to additional information such as laboratory measurements and other types of theory based calculations. With respect to qualitative analysis, these spectra provide for the molecular level interpretation of response structure. The DFT software GAUSSIAN was used for the calculations of ground state resonance structure presented here.

15. SUBJECT TERMS

Density functional theory (DFT)
Dielectric functions
Explosives

16. SECURITY CLASSIFICATION OF:			**17. LIMITATION OF ABSTRACT**	**18. NUMBER OF PAGES**	**19a. NAME OF RESPONSIBLE PERSON**
a. REPORT	**b. ABSTRACT**	**c. THIS PAGE**			Samuel G. Lambrakos
Unclassified	Unclassified	Unclassified	UU	49	**19b. TELEPHONE NUMBER** *(include area code)* (202) 767-2601

Standard Form 298 (Rev. 8-98)
Prescribed by ANSI Std. Z39.18

Contents

Introduction

A significant aspect of using response spectra calculated by density functional theory, DFT, for the direct construction of dielectric response functions is that it adopts the perspective of computational physics, according to which a numerical simulation represents another source of "experimental" data. This perspective is significant in that a general procedure may be developed for construction of dielectric response functions using DFT calculations as a quantitative initial estimate of spectral response features for subsequent adjustment with respect to additional information such as experimental measurements and other types of theory based calculations. That is to say, for the purpose of simulating many electromagnetic response characteristics of materials, DFT is sufficiently mature for the purpose of generating data complementing, as well as superseding, experimental measurements.

In the case of THz excitation of materials, the procedure of using response spectra calculated using DFT, which is associated with ground state resonance structure, for the direct construction of permittivity functions is well posed owing to the physical characteristic of THz excitation. In particular, it is important to note that the procedure for constructing a permittivity function using response spectra calculated using DFT is physically consistent with the characteristically linear response associated with THz excitation of molecules. Accordingly, one observes a correlation between the advantages of using THz excitation for detection of IEDs (and ambient materials) and those for its numerical simulation based on DFT. Specifically, THz excitation is associated with frequencies that are characteristically perturbative to molecular states, in contrast to frequencies that can induce appreciable electronic state transitions. Of course, the practical aspect of the perturbative character of THz excitation for detection is that detection methodologies can be developed which do not damage materials under examination. The perturbative character of THz excitation with respect to molecular states has significant implications with respect to its numerical simulation based on DFT. It follows then that, owing to the perturbative character of THz excitation, which is characteristically linear, one is able to make a direct association between local oscillations about ground-state minima of a given molecule and THz excitation spectra.

In what follows, calculations are presented of ground state resonance structure associated with molecular clusters of RDX. This resonant structure is for the construction of parameterized dielectric response functions for excitation by electromagnetic waves at compatible frequencies. For this purpose the DFT software GAUSSIAN09 (G09) was adopted [1].

The organization of the subject areas presented here are as follows. First, a general review of the elements of vibrational analysis using DFT that are relevant for the calculation of absorption spectra is presented. Second, a general review is presented concerning the formal structure of permittivity functions in terms of analytic function representations. An understanding of the formal structure of permittivity functions in terms of both physical consistency and causality is important for post-processing of DFT calculations for the purpose of constructing permittivity functions. Third, information concerning the ground state resonance structure of molecular clusters of RDX, PETN and TNT, which are obtained using DFT, is presented as a set of case studies. This information consists of the ground state molecular geometry and response spectra for isolated molecules.

Manuscript approved December 7, 2011.

Construction of Dielectric Response Functions using DFT

Density Functional Theory

The application of density functional theory (DFT) and related methodologies for the determination of electromagnetic response characteristics is important for the analysis of parameter sensitivity. That is to say, many characteristics of the electromagnetic response of a given material may not be detectable, or in general, not relevant for detection. Accordingly, sensitivity analyses concerning the electromagnetic response of layered composite systems can adopt the results of simulations using DFT, and related methodologies, to provide realistic limits on detectability that are independent of a specific system design for IED detection. In addition, analysis of parameter sensitivity based on atomistic response characteristics of a given material, obtained by DFT, provide for an "optimal" best fit of experimental measurements for the construction of permittivity functions. It follows that within the context of parameter sensitivity analysis, data obtained by means of DFT represents a true complement to data that has been obtained by means of experimental measurements.

The DFT software GAUSSIAN09 (G09) can be used to compute an approximation of the IR absorption spectrum of a molecule or molecules [1]. This program calculates vibrational frequencies by determining second derivatives of the energy with respect to the Cartesian nuclear coordinates, and then transforming to mass-weighted coordinates at a stationary point of the geometry. [2]. The IR absorption spectrum is obtained using density functional theory to compute the ground state electronic structure in the Born-Oppenheimer approximation using Kohn-Sham density functional theory [3-7]. GAUSSIAN uses specified orbital basis functions to describe the electronic wavefunctions and density. For a given set of nuclear positions, the calculation directly gives the electronic charge density of the molecule, the potential energy *V*, and the displacements in Cartesian coordinates of each atom. The procedure for vibrational analysis followed in GAUSSIAN is that described in [8]. Reference [9] presents a fairly detailed review of this procedure. A brief description of this procedure is as follows.

The procedure followed by GAUSSIAN is based on the fact the vibrational spectrum depends on the Hessian matrix $\mathbf{f}_{\mathrm{CART},}$ which is constructed using the second partial derivatives of the potential energy *V* with respect to displacements of the atoms in Cartesian coordinates. Accordingly, the elements of the *3N* x *3N* matri*x* $\mathbf{f}_{\mathrm{CART}}$ are given by

$$f_{\mathrm{CART}ij} = \left(\frac{\partial^2 V}{\partial \xi_i \partial \xi_j} \right)_0 \tag{1}$$

where $\{\xi_1,\xi_2,\xi_3,\xi_4,\xi_5,\xi_6,...,\xi_{3N}\} = \{\Delta x_1,\Delta y_1,\Delta z_1,\Delta x_2,\Delta y_2,\Delta z_2,...,\Delta z_N\}$, which are displacements in Cartesian coordinates, and *N* is the number of atoms. As discussed above, the zero subscript in Eq.(1) indicates that the derivatives are taken at the equilibrium positions of the atoms, and that the first derivatives are zero. Given the Hessian matrix defined by Eq.(1) the operations for calculation of the vibrational spectrum require that the Hessian matrix Eq.(1) be transformed to mass-weighted Cartesian coordinates according to the relation

$$f_{\mathrm{MWC}ij} = \frac{f_{\mathrm{CART}ij}}{\sqrt{m_i m_j}} = \left(\frac{\partial^2 V}{\partial q_i \partial q_j} \right)_0 \tag{2}$$

where $\{q_1,q_2,q_3,q_4,q_5,q_6,...,q_{3N}\} = \left\{\sqrt{m_1}\Delta x_1,\sqrt{m_1}\Delta y_1,\sqrt{m_1}\Delta z_1,\sqrt{m_2}\Delta x_2,\sqrt{m_2}\Delta y_2,\sqrt{m_2}\Delta z_2,...,\sqrt{m_N}\Delta z_N\right\}$ are the mass-weighted Cartesian coordianates. GAUSSIAN computes the energy second derivatives Eq.(2), thus computing the forces for displacement perturbations of each atom along each Cartesian direction. The first derivatives of the dipole moment with respect to atomic positions $\partial\bar{\mu}/\partial\xi_i$ are also computed. Each vibrational eigenmode leads to one peak in the absorption spectrum, at a frequency equal to the

mode's eigenfrequency ν_{n0}. The absorption intensity corresponding to a particular eigenmode *n* whose eigenfrequency is ν_{n0} is given by

$$I_n = \frac{\pi}{3c}\left|\sum_{i=1}^{3N}\frac{\partial\vec{\mu}}{\partial\xi_i}l_{\mathrm{CART}in}\right|^2, \tag{3}$$

where $\mathbf{l}_{\mathrm{CART}}$ is the matrix whose elements are the displacements of the atoms in Cartesian coordinates. The matrix $\mathbf{l}_{\mathrm{CART}}$ is determined by the following procedure. First,

$$\mathbf{l}_{\mathrm{CART}} = \mathbf{M}\mathbf{l}_{\mathrm{MWC}}, \tag{4}$$

where $\mathbf{l}_{\mathrm{MWC}}$ is the matrix whose elements are the displacements of the atoms in mass-weighted Cartesian coordinates and **M** is a diagonal matrix defined by the elements

$$M_{ii} = \frac{1}{\sqrt{m_i}}. \tag{5}$$

Proceeding, $\mathbf{l}_{\mathrm{MWC}}$ is the matrix needed to diagonalize $\mathbf{f}_{\mathrm{MWC}}$ defined by Eq.(2) such that

$$(\mathbf{l}_{\mathrm{MWC}})^{\mathrm{T}}\,\mathbf{f}_{\mathrm{MWC}}(\mathbf{l}_{\mathrm{MWC}}) = \Lambda, \tag{6}$$

where Λ is the diagonal matrix with eigenvalues λ_i. The procedure for diagonalizing Eq.(6) consists of the operations

$$\mathbf{f}_{\mathrm{INT}} = (\mathbf{D})^{\mathrm{T}}\,\mathbf{f}_{\mathrm{MWC}}(\mathbf{D}) \tag{7}$$

and

$$(\mathbf{L})^{\mathrm{T}}\,\mathbf{f}_{\mathrm{MWC}}(\mathbf{L}) = \Lambda, \tag{8}$$

where **D** is a matrix transformation to coordinates where rotation and translation have been separated out and **L** is the transformation matrix composed of eigenvectors calculated according to Eq.(8). The eigenfrequencies in units of (cm^{-1}) are calculated using the eigenvalues λ_n by the expression

$$\nu_{n0} = \frac{\sqrt{\lambda_n}}{2\pi c}, \tag{9}$$

where *c* is the speed of light. The elements of $\mathbf{l}_{\mathrm{CART}}$ are given by

$$l_{\mathrm{CART}ki} = \sum_{j=1}^{3N}\frac{D_{kj}L_{ji}}{\sqrt{m_j}}, \tag{10}$$

where *k, i=1,…, 3N,* and the column vectors of these elements are the normal modes in Cartesian coordinates.

The intensity Eq.(3) must then be multiplied by the number density of molecules to give an absorption strength. It follows that the absorption spectrum calculated by GAUSSIAN is a sum of delta functions whose positions and magnitudes correspond to the vibrational frequencies and magnitudes, respectively. In principle, however, these spectral components must be broadened and shifted to account for anharmonic effects such as finite mode lifetimes and inter-mode couplings.

Dielectric Response Functions

The general approach of constructing permittivity functions according to the best fit of available data for given material corresponding to many different types of experimental measurements has been typically the dominant approach. The present study extends this approach in that calculations of electromagnetic response based on DFT are also adopted as data for construction of permittivity functions. The inclusion of this type of information is significant for accessing what spectral response features at the molecular level are actually detectable with respect to a given set of detection parameters. Accordingly, permittivity functions having been constructed using DFT calculations provide a quantitative correlation between macroscopic material response and molecular structure. Within this context it is not important that the permittivity function be quantitatively accurate for the purpose of being adopted as input for system simulation. Rather, it is important that the permittivity function be qualitatively accurate in terms of specific dielectric response features for the purpose of sensitivity analysis, which is relevant for the assessment of absolute detectability of different types of molecular structure with respect to a given set of detection parameters. That is to say, permittivity functions that have been determined using DFT can provide a mechanistic interpretation of material response to electromagnetic excitation that could establish the well posedness of a given detection methodology for detection of specific molecular characteristics. Within the context of practical application, permittivity functions having been constructed according to the best fit of available data would be "correlated" with those obtained using DFT for proper interpretation of permittivity-function features. Subsequent to establishment of good correlation between DFT and experiment, DFT calculations can be adopted as constraints for the purpose of constructing permittivity functions, whose features are consistent with molecular level response, for adjustment relative to specific sets of either experimental data or additional molecular level information.

The construction of permittivity functions using DFT calculations involves, however, an aspect that requires serious consideration. This aspect concerns the fact that a specific parametric function representation must be adopted. Accordingly, any parametric representation, i.e., parameterization, adopted for permittivity-function construction must be physically consistent with specific molecular response characteristics, while limiting the inclusion of feature characteristics that tend to mask response signatures that may be potentially detectable.

In principle, parameterizations are of two classes. One class consists of parameterizations that are directly related to molecular response characteristics. This class of parameterizations would include spectral scaling and width coefficients. The other class consists of parameterizations that are purely phenomenological and are structured for optimal and convenient best fits to experimental measurements. A sufficiently general parameterization of permittivity functions is given by Drude-Lorentz approximation [10]

$$\varepsilon(\nu) = \varepsilon'(\nu) + i\varepsilon''(\nu) = \varepsilon_\infty + \sum_{n=1}^{N} \frac{\nu_{np}^2}{(\nu_{no}^2 - \nu^2) - i\gamma_n \nu} \ , \tag{11}$$

where ν_{np} and γ_n are the spectral scaling and width of a resonance contributing to the permittivity function. The permittivity ε_∞ is a constant since the dielectric response at high frequencies is substantially detuned from the probe frequency. The real and imaginary parts, $\varepsilon_r(\nu)$ and $\varepsilon_i(\nu)$, respectively, of the permittivity function can be written separately as

$$\varepsilon_r(\nu) = \varepsilon_\infty + \sum_{n=1}^{N} \frac{\nu_{np}^2(\nu_{no}^2 - \nu^2)}{(\nu_{no}^2 - \nu^2)^2 + \gamma_n^2 \nu^2} \quad \text{and} \quad \varepsilon_i(\nu) = \sum_{n=1}^{N} \frac{\nu_{np}^2 \gamma_n \nu}{(\nu_{no}^2 - \nu^2)^2 + \gamma_n^2 \nu^2} \ . \tag{12}$$

With respect to practical application, the absorption coefficient α and index of refraction n_r, given by

$$\alpha = \frac{4\pi\nu}{\sqrt{2}}\left[-\varepsilon_r + \sqrt{\varepsilon_r^2 + \varepsilon_i^2}\right]^{1/2} \quad \text{and} \quad n_r = \frac{1}{\sqrt{2}}\left[\varepsilon_r + \sqrt{\varepsilon_r^2 + \varepsilon_i^2}\right]^{1/2}, \tag{13}$$

respectively, provide direct relationships between calculated quantities obtained by DFT and the "conveniently measurable" quantities α and n_r. It is significant to note that in what follows, the absorption coefficient α is determined using DFT calculated spectra in the same spirit as for its measurement in the laboratory. Although permittivity functions $\varepsilon(\nu)$ are not determined explicitly in the present study, it must be kept in mind that the ultimate construction of these functions is necessary for using DFT calculated spectra to model the dielectric response of complex composite materials and associated detector designs [11].

Ground State Resonance Structure of Molecular Clusters of RDX

In this section are presented the results of computational experiments using DFT concerning molecular clusters of RDX. These results include the relaxed or equilibrium configuration of a single isolated molecule of RDX (see Table 1) and ground-state oscillation frequencies and IR intensities for this configuration, which are calculated by DFT according to the frozen phonon approximation (see Table 2). The ground state resonance structure for a single isolated molecule of RDX is adopted as a reference for analysis of spectral features associated with molecular clusters of different sizes. For these calculations geometry optimization and vibrational analysis was effected using the DFT model B3LYP [12, 13] and basis function 6-311G(2d,2p) [14,15]. According to the specification of this basis function, (2d,2p) designates polarization functions having 2 sets of d functions for heavy atoms and 2 sets of p functions for hydrogen atoms [16]. A schematic representation of the molecular geometry of a single isolated molecule of RDX is shown in Fig.(1). A schematic representation of molecular geometries of molecular clusters consisting of 2, 4 and 6 molecules are shown in Figs. (2), (3) and (4), respectively. It is significant to note that the relative positions of the molecules associated with each of the molecular clusters is according to crystallographic structure conditions that would be associated with bulk material. In particular, the crystal structure of α–RDX, whose CCDC reference code is CTMTNA, has been investigated by C. S. Choi and E. Prince [17]. The space group for this crystal structure is ***P****bca* (symmetry operators are x, y, z; 1/2-x, -y, 1/2+z; 1/2+x, 1/2-y, -z; -x, 1/2+y, 1/2-z; -x, -y, -z; 1/2+x, y, 1/2-z; 1/2-x, 1/2+y, z; x, 1/2-y, 1/2+z), and the unit cell constants are a=13.182, b=11.574, c=10.709, α=0.00, β=90.00, γ=90.00 and density 1.806 g/cm^3. The ground-state oscillation frequencies and IR intensities for the different molecular clusters of RDX, corresponding to their relaxed equilibrium configurations, are calculated by DFT according to the frozen phonon approximation. In the cases of molecular clusters of 2, 4 and 6 molecules, these values are given in Tables 3, 4 and 5, respectively. The DFT model and basis function used for these calculations are the same as those used for the single isolated molecule of RDX. Two programs, ConQuest and Mercury [18], have been used for searching the Cambridge Structural Database (CSD), visualizing database entries, RDX, and creating the n-molecule clusters. We have considered the interactions and forces between the single molecule and its neighborhood when we created the cluster. Hydrogen bonding between the molecules is important for establishing the cluster.

The DFT calculated absorption spectra given in tables 3, 4 and 5 provide information for analysis of dielectric response with respect to the size of molecular clusters, i.e., the denumeration of ground state resonance modes and estimates of molecular level dielectric response structure. The construction of permittivity functions using the DFT calculated absorption spectra follows the same

procedure as that applied for the construction of permittivity functions using experimentally measured absorption spectra, but with the addition of certain constraint conditions. Accordingly, construction of permittivity functions using either DFT or experimentally measured absorption spectra requires parameterizations that are in terms of physically consistent analytic function representations such as the Drude-Lorentz model, i.e., Eqs.(11) and (12). Although the formal structure of permittivity functions constructed using DFT and experimental measurements are the same, their interpretation with respect to parameterization is different for each case.

Table 1. Atomic positions of RDX (Å) after geometry optimization.

Atomic number	X	Y	Z	Atomic number	X	Y	Z
7	1.177132	-0.800831	0.102459	8	-1.148702	1.861918	2.523892
7	0.102459	1.177132	-0.800831	8	3.333613	-0.184585	0.086238
7	-0.800831	0.102459	1.177132	8	0.086238	3.333613	-0.184585
7	2.436639	-0.679768	0.742611	8	-0.184585	0.086238	3.333613
7	0.742611	2.436639	-0.679768	1	-1.515435	1.871323	0.32473
7	-0.679768	0.742611	2.436639	1	0.32473	-1.515435	1.871323
6	-1.083455	0.93108	0.011066	1	1.871323	0.32473	-1.515435
6	0.011066	-1.083455	0.93108	1	-1.794386	0.385919	-0.609699
6	0.93108	0.011066	-1.083455	1	-0.609699	-1.794386	0.385919
8	2.523892	-1.148702	1.861918	1	0.385919	-0.609699	-1.794386
8	1.861918	2.523892	-1.148702				

Before proceeding with further discussion concerning various features of dielectric response with respect to the size of molecular clusters, it is necessary to again indicate two general goals underlying the DFT calculations presented here and in related studies. These goals are, first, to obtain an understanding of the physical nature underlying the various spectral features associated with the dielectric response of materials, and second, the construction of dielectric response functions for use in quantitative simulation of detector designs and their associated detection scenarios. With respect to the second goal, the DFT calculated absorption spectra given above are to be considered the results of computational experiments for the purpose of being correlated, as well as combined, with other absorption spectra, which may be the results of both computational experiments and laboratory measurements. Accordingly, the dielectric response of a molecular cluster consisting of a given number of molecules can be associated with response features that are intermediate between that of isolated molecules and that of the bulk lattice response. It follows that for analysis of spectra, permittivity functions for finite size molecular clusters can be adopted for use in effective medium theories in order to model the dielectric response of composite materials. This follows in that a composite material may be characterized by a non-interacting uniform distribution of finite-size molecular clusters within a host material. Models based on this type of characterization are for further investigation.

Proceeding, shown in Figs. 6, 7, 8 and 9 are calculated IR intensities for a single isolated molecule, 2-molecule cluster, 4-molecule cluster and 6-molecule cluster, respectively. Referring to Figs. 10 and 11, one notes continuous spectra consisting of a superposition of essentially Lorenzian functions of various heights and widths, which have been constructed using discrete spectra. Although the primarily purpose of this type of construction within GAUSSIAN is for the purpose of enhanced visualization of spectral features, it is significant to note that this operation represents an estimation of the characteristic scaling and width of resonances contributing the dielectric response. With respect to

the interrelationship between the absorption coefficient α and the permittivity function $\varepsilon(\nu)$ defined by Eqs.(11), (12) and (13), this represents an estimation of the parameters ν_{np} and γ_n, which are the spectral scaling and width of a resonance contributing to the permittivity function. For qualitative comparison of spectral features this type of estimate should be sufficient. For the construction of permittivity functions using DFT calculated spectra for subsequent use for quantitative simulation, it is more appropriate, however, to assume the parameters ν_{np} and γ_n adjustable, i.e., to be assigned values according to additional information.

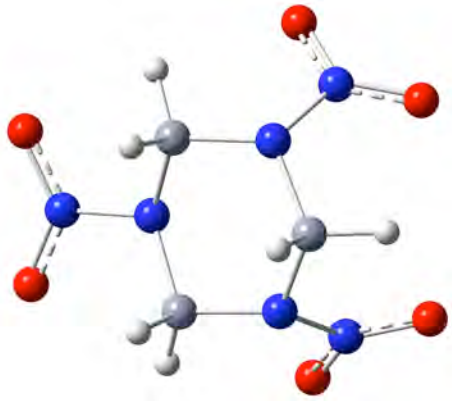

Figure 1. Molecular Geometry of RDX.

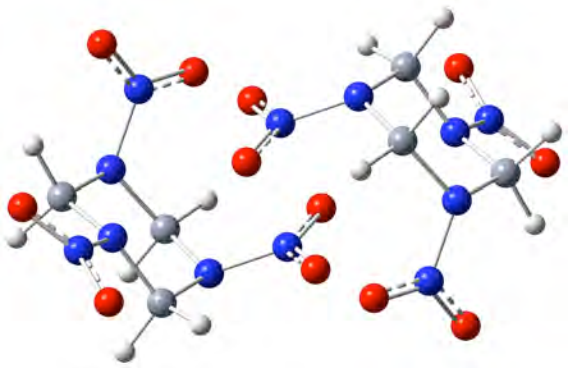

Figure 2. Molecular Geometry of 2-Molecule Cluster of RDX.

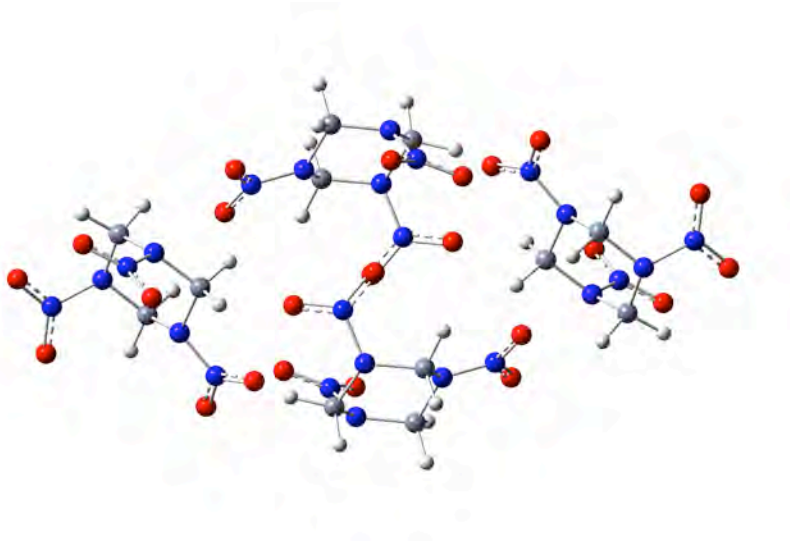

Figure 3. Molecular Geometry of 4-Molecule Cluster of RDX.

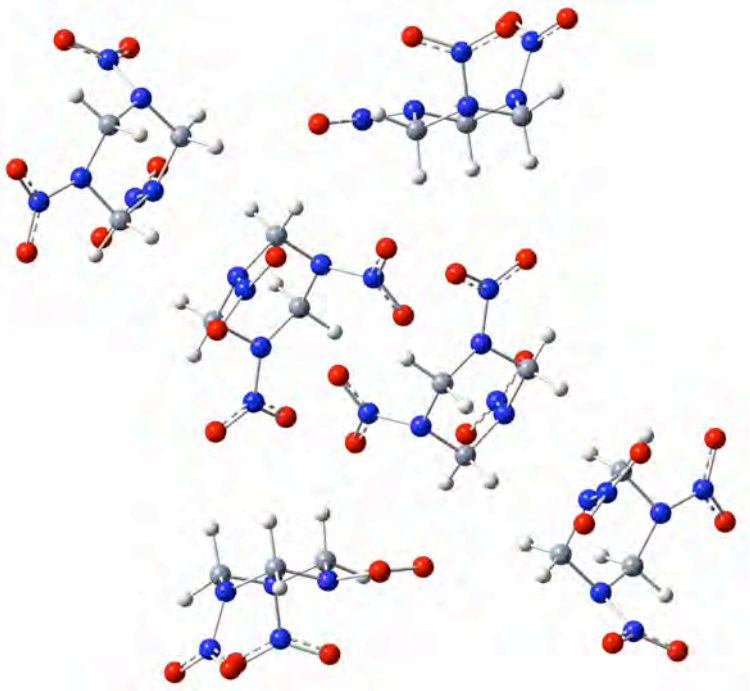

Figure 4. Molecular Geometry of 6-Molecule Cluster of RDX.

Table 2. Oscillation frequencies and IR intensities for single isolated molecule of RDX.

Frequency cm^{-1}	Intensity (km/mol)	Frequency cm^{-1}	Intensity (km/mol)	Frequency cm^{-1}	Intensity (km/mol)	Frequency cm^{-1}	Intensity (km/mol)
42.2254	0.0182	584.6074	10.0692	1024.3428	168.8792	1467.5898	39.3506
56.9758	2.521	592.499	0.9828	1044.7485	37.0924	1482.6062	2.6857
61.6615	1.2995	613.8533	15.7407	1161.983	1.5664	1499.7183	46.3106
74.6522	0.0198	656.5469	0.0877	1237.517	20.8868	1663.0582	150.5
93.4908	0.1868	681.3616	4.103	1247.1127	39.6523	1683.8234	223.9439
114.9468	0.0237	764.6259	1.6194	1270.7874	6.6058	1701.8562	377.1413
210.9971	7.4608	773.8667	0.4212	1270.868	70.4238	3016.3838	4.5269
222.2105	1.3202	783.2278	2.4613	1310.4281	336.5103	3018.0322	39.0865
290.7538	0.001	808.6349	61.0009	1311.0815	125.0556	3082.2839	15.4483
327.5155	2.1052	860.6995	34.5479	1346.6562	61.2854	3216.2893	12.8591
378.0279	0.0344	874.637	5.7883	1361.4716	4.2675	3221.1511	12.1171
410.0315	0.3607	902.7032	38.0133	1370.1674	132.9406	3222.6191	7.9466
413.9516	9.1916	922.3189	232.1041	1376.7496	6.1702		
439.9936	9.9427	947.0868	178.6166	1410.854	11.1317		
472.7935	15.7833	961.2388	110.5947	1425.8851	95.0582		

Table 3. Oscillation frequencies and IR intensities for 2-molecule cluster of RDX.

Frequency cm^{-1}	Intensity (km/mol)	Frequency cm^{-1}	Intensity (km/mol)	Frequency cm^{-1}	Intensity (km/mol)	Frequency cm^{-1}	Intensity (km/mol)
14.9682	0.2645	410.6108	18.9557	928.1564	0	1380.856	0
26.1434	2.6138	411.9108	0	933.6769	388.6451	1380.9839	14.262
29.3972	0	431.3649	26.9949	947.9423	0	1413.2908	0
35.0656	1.686	431.9862	0	951.4927	389.1337	1413.4794	26.0848
48.6587	0	462.2036	0	965.8482	0	1426.1849	170.412
48.8051	0.8348	462.2959	24.2307	967.4657	120.6746	1426.6543	0
52.4387	0	588.422	20.4808	1032.6176	0	1467.2236	97.7646
58.4871	6.7772	588.5022	0	1033.149	340.5911	1467.9124	0
60.7165	0	602.5717	0	1047.2354	0	1485.0341	7.5186
69.1863	0	602.7465	4.1501	1048.9814	84.5362	1485.3751	0
86.8182	2.2742	615.5301	0	1169.7606	0	1501.0522	94.1043
90.5851	0	615.8413	33.0986	1169.8094	1.5371	1501.2987	0
91.258	0.4119	661.6494	0.6713	1246.179	0	1657.328	179.9943
96.1505	0	661.679	0	1246.2902	38.9162	1658.2531	0
100.3821	0.172	685.3188	0	1257.6866	0	1662.3564	0
113.2955	0	686.3688	5.5564	1258.2448	66.1412	1677.2478	601.3396
124.3702	0.4582	766.0924	16.4961	1266.9543	23.0611	1695.8433	0
134.6481	0	766.169	0	1266.9575	0	1696.4061	565.5932
212.6795	13.8607	770.9064	1.8229	1272.184	0	3009.2444	38.2081
213.2402	0	773.5341	0	1272.4142	135.649	3009.2595	0
215.3385	0	778.6134	0	1306.4919	564.6394	3013.1033	77.6467
221.1027	2.4114	779.4847	10.866	1307.7988	0	3013.2798	0
293.015	0	803.2578	164.0284	1310.0482	0	3076.2737	38.0099
293.6024	0.0206	806.1595	0	1312.1539	294.3002	3076.3501	0
327.11	7.3232	862.963	74.0208	1348.7789	0	3215.1035	0
327.3015	0	864.6105	0	1350.2686	101.1641	3215.1763	23.6244
374.0134	0	876.7775	0	1363.9604	0	3218.981	0
374.1297	0.0955	877.259	4.6032	1364.0728	7.9788	3219.0559	28.491
406.1292	0	901.3114	68.6632	1370.1343	0	3220.7827	17.6924
406.6222	2.8765	901.419	0	1374.3319	331.9773	3220.7993	0

Table 4. Oscillation frequencies and IR intensities for 4-molecule cluster of RDX.

Frequency cm^{-1}	Intensity (km/mol)	Frequency cm^{-1}	Intensity (km/mol)	Frequency cm^{-1}	Intensity (km/mol)	Frequency cm^{-1}	Intensity (km/mol)
5.9417	0.8932	218.3001	0	681.218	5.0704	1049.8677	216.8569
11.2558	0	227.3244	3.589	681.2275	0	1050.019	0
12.1643	1.8844	227.3429	0	685.1279	0	1050.8359	183.4953
17.1016	0.7561	292.3184	0	686.3152	2.8861	1057.8466	0
18.0733	0	292.3708	0.0697	763.4879	2.4633	1059.7562	409.959
22.1499	0.8163	297.7226	0	763.5641	0	1152.1003	0
28.6989	0	298.443	0.5903	765.5928	0	1152.1033	3.507
30.4139	3.2113	334.8958	0	765.6132	3.4463	1165.8265	0
30.6346	0	334.9269	6.8163	769.1978	7.4405	1165.8674	2.651
32.9922	5.0297	336.7472	5.1234	771.9295	0	1241.8436	129.8683
34.6379	2.1739	336.9161	0	775.0354	0	1242.0962	0
37.3103	0	373.1536	0	775.0493	24.4915	1243.5063	0
43.0674	0	373.2618	0.3094	775.3522	0	1243.582	64.6015
46.2171	0.254	382.1399	0.0763	775.3527	0.5402	1250.0132	0
48.6162	0	382.1516	0	785.7931	0	1250.8424	130.1652
53.1727	0	404.5152	38.1485	785.8521	23.2646	1260.1033	0
53.5529	1.984	405.4077	0	799.5599	113.6132	1260.714	52.2322
55.7237	0.3531	409.244	0	801.5757	0	1267.402	28.1434
56.7595	0	409.8144	0.4239	807.4271	177.408	1267.7118	0
59.5683	0	411.4004	2.0287	807.6755	0	1270.1116	0
63.8558	2.6444	411.5578	0	853.126	0	1271.1813	226.9784
64.0555	0	415.4892	26.128	853.1605	70.288	1274.3192	109.6892
64.2175	2.9595	415.5214	0	857.0704	37.5648	1274.6527	0
68.6191	0	428.8975	22.651	857.843	0	1279.0389	0
72.4516	8.4016	429.463	0	874.676	0	1279.0677	13.0795
75.5401	0	452.5779	59.8655	875.0377	19.4847	1305.5767	304.1009
79.1997	1.2599	452.8454	0	875.1404	3.0135	1308.7438	0
80.1933	0	468.1582	0	875.1481	0	1311.9091	0
83.536	7.8691	468.3085	13.3874	895.7402	78.105	1312.7611	288.9891
90.1537	0	482.5359	74.0979	897.0327	0	1313.2223	0
93.6963	6.4259	482.6726	0	903.7427	29.171	1314.9039	986.756
102.0439	1.0454	589.0296	0	903.7535	0	1318.5479	0
102.3205	0	589.1119	20.029	925.3393	250.4504	1320.8827	487.5419
114.0193	0	592.5375	1.1143	925.3761	0	1348.9429	0
119.1062	0.1219	592.5639	0	925.9388	0	1350.5767	152.6872
120.8635	0	596.34	29.464	930.7203	475.2726	1353.9634	0
120.9227	0.0928	596.5048	0	943.2045	0	1354.9141	175.168
124.0232	0.3339	604.0503	0	945.0859	397.0026	1367.0991	0
124.0666	0	604.199	0.7334	954.5926	468.9313	1367.1254	22.7386
128.5985	0	614.1897	0	955.4067	0	1368.368	0
145.2666	0	615.0315	78.044	968.2669	0	1368.5292	1.3385
147.8037	1.5142	619.4185	0	970.01	145.2878	1377.3337	0
187.6243	0	619.5198	45.152	970.8496	0	1378.8676	210.1102
193.0925	1.2304	657.7129	0.3953	972.0773	116.258	1383.1447	0
212.9453	9.0403	657.7307	0	1048.3354	0	1384.4601	128.5912
212.9988	0	658.9496	5.8763	1048.5754	113.7712	1387.149	0
217.5362	17.2925	659.1081	0	1048.6093	0	1387.1785	19.1128

Table 4. (continued)

Frequency cm^{-1}	Intensity (km/mol)	Frequency cm^{-1}	Intensity (km/mol)	Frequency cm^{-1}	Intensity (km/mol)	Frequency cm^{-1}	Intensity (km/mol)
1388.3368	0	1482.5695	0	1696.0105	0	3109.188	6.2155
1389.1818	197.8481	1486.8042	0	1696.0919	958.9728	3216.2964	0
1418.2656	0	1486.9224	6.0855	1697.5343	0	3216.3967	23.3328
1418.4442	69.7893	1497.5839	99.1629	1698.3257	435.5343	3218.6729	0
1419.0931	0	1497.9727	0	3028.8118	34.3859	3218.7385	66.0843
1419.1238	20.7794	1506.0269	71.3172	3028.8286	0	3221.2642	0
1427.403	0	1506.0958	0	3033.7673	45.2205	3221.2849	71.082
1429.0955	182.339	1614.6718	172.3449	3033.8721	0	3223.749	32.0502
1433.496	329.1365	1618.0834	0	3057.082	0	3223.7571	0
1434.8369	0	1622.3704	0	3057.0933	2.066	3225.3008	25.2271
1456.7389	112.6976	1624.3489	520.7316	3062.8665	11.5487	3225.3062	0
1457.354	0	1640.2415	0	3062.8721	0	3228.2629	28.9712
1475.7458	0	1652.6211	494.1416	3095.7844	13.1672	3228.2712	0
1475.816	45.857	1675.8097	0	3095.8081	0		
1482.1519	14.8717	1675.9667	267.4778	3109.1875	0		

Table 5. Oscillation frequencies and IR intensities for 6-molecule cluster of RDX.

Frequency cm^{-1}	Intensity (km/mol)	Frequency cm^{-1}	Intensity (km/mol)	Frequency cm^{-1}	Intensity (km/mol)	Frequency cm^{-1}	Intensity (km/mol)
4.3759	0.052	81.9255	0	382.4558	0	657.5724	0.0572
6.3809	0.4456	86.685	8.0455	382.4635	0.184	663.3732	0
6.6603	0	90.8211	0	396.9643	14.1359	663.6753	4.3512
8.3081	1.5655	92.2727	12.5623	397.1129	0	680.6752	0
11.3305	1.1677	94.7594	0.7639	401.1577	6.1866	680.6866	4.1544
11.4291	0	94.7711	0	401.2039	0	686.9826	0
13.5796	0	100.6031	0	406.1711	0	687.2872	0.3263
15.5115	0	101.9998	1.2895	406.3565	19.1602	690.2896	0
18.5873	1.6704	114.5513	0	409.9726	1.8507	690.3004	9.8633
20.9307	3.5563	118.8257	0.393	410.033	0	764.5281	28.3151
21.1463	0	119.7657	0	413.1681	0	764.6277	0
21.7823	1.194	121.2679	0	413.1752	19.0126	765.3242	2.2033
24.7982	0	121.3376	0.0639	414.8473	28.0452	765.3998	0
25.0879	1.4846	122.214	0.4227	414.9183	0	766.1323	10.3475
28.8329	0	125.993	0	431.0954	19.0787	766.535	0
29.6123	2.1614	131.7202	2.9282	431.6634	0	767.5119	6.1219
31.0821	2.4051	131.7806	0	439.8429	0	768.0571	0
31.4382	0	136.3106	0	439.8558	15.3285	770.9393	9.0595
33.4071	0	138.8273	0.5152	451.8383	61.9663	771.0958	0
34.9247	4.8311	187.4796	0	452.0278	0	774.2007	33.164
34.9452	0	191.0382	1.5234	471.8306	0	774.2167	0
43.3381	0.5939	209.4877	17.7486	472.242	15.1678	774.9939	0
43.4133	0	209.5666	0	475.251	24.5623	774.9948	0.4784
44.9009	0	212.7895	9.2759	475.2595	0	782.3235	0
48.2995	0.1558	212.8572	0	482.1034	75.0025	782.3255	7.2197
49.2102	3.4005	216.833	5.2226	482.224	0	784.3684	0
50.9147	0	216.897	0	585.1803	25.4609	784.4365	18.3544
53.2002	0	218.1313	11.6504	585.2159	0	798.4154	112.0094
55.3069	0.3144	218.4937	0	588.9885	0	801.8206	0
56.3097	0	226.7978	4.7359	589.0536	21.5489	806.6279	169.7447
59.1625	5.991	226.9038	0	592.4738	0	806.8649	0
59.8489	0	289.7068	0	592.4745	0.1328	807.9775	120.8904
61.5608	5.0124	289.7116	0.0827	598.1579	26.6417	808.0478	0
63.2771	0.8748	291.2965	0	598.1992	0	850.2579	0
63.3703	0	291.5054	0.0912	599.2144	0	850.3431	74.6704
64.3256	1.8769	297.7133	0	599.2544	21.2304	855.7887	39.2629
64.8365	0	297.9614	1.3903	609.5693	0	856.9945	0
65.9391	2.4496	326.2533	0	609.707	6.4886	860.7501	56.5966
67.77	0	326.257	4.2363	614.2649	56.2976	860.8075	0
69.6183	0	333.3926	0	614.3472	0	874.3911	0
74.2641	4.8827	333.9757	4.8618	618.3128	0	874.3951	8.7236
75.2432	0	335.076	8.9796	619.3108	85.1984	875.2409	5.9103
76.0726	4.2221	335.7368	0	619.7584	52.6792	875.2426	0
79.8592	0	365.5461	1.7189	619.8212	0	877.4122	0
80.8216	1.4527	365.6725	0	655.3927	9.2644	877.8359	14.8603
80.8688	0	373.5711	0	655.399	0	898.2481	43.774
81.4978	0.2355	373.5727	0.5468	657.5675	0	898.3571	0

Table 5. (continued)

Frequency cm^{-1}	Intensity (km/mol)	Frequency cm^{-1}	Intensity (km/mol)	Frequency cm^{-1}	Intensity (km/mol)	Frequency cm^{-1}	Intensity (km/mol)
898.9678	114.2656	1249.6028	0	1384.7289	0	1673.2216	1253.6383
899.6584	0	1252.2239	0	1386.7623	54.0952	1677.5648	254.4055
903.7786	0	1253.5337	140.7511	1386.9449	0	1677.5771	0
903.7878	40.4836	1259.2854	0	1387.2804	311.9294	1696.2489	0
925.1438	0	1259.7135	74.642	1387.6086	0	1696.2622	751.9892
925.2002	292.8446	1268.1906	19.3053	1387.6719	13.3364	1698.1921	0
931.0855	649.434	1268.2472	0	1414.9059	44.1271	1698.2057	641.3516
931.3673	0	1268.922	47.0974	1414.9625	0	3023.3391	21.6024
937.9984	0	1268.9448	0	1418.0494	65.8201	3023.3445	0
941.9125	342.7514	1273.0648	142.252	1418.2875	0	3027.7644	0
947.154	0	1273.0767	0	1419.486	1.4432	3027.7686	39.5879
948.7826	415.3135	1275.387	0	1419.5223	0	3038.7473	16.1057
950.1349	316.6856	1275.6105	233.769	1425.1407	235.0826	3038.76	0
950.1881	0	1278.2577	0	1425.2646	0	3043.4661	31.0481
954.576	453.1379	1278.3093	103.4302	1429.217	0	3043.5422	0
955.4264	0	1281.2936	0	1431.4359	198.5826	3062.6191	8.9564
966.3974	0	1281.2948	11.3502	1434.2299	374.2726	3062.6216	0
966.5695	114.222	1301.0441	0	1435.7983	0	3066.1562	0
969.9396	0	1302.1788	192.7808	1457.8159	193.8634	3066.1794	3.3107
971.1288	151.9144	1309.0847	272.2128	1458.1257	0	3102.0098	10.9209
975.6687	0	1309.2377	0	1461.3976	17.8474	3102.01	0
977.1353	79.7326	1312.2554	286.1903	1461.6547	0	3107.6062	0
1024.5593	0	1312.9231	0	1475.097	0	3107.616	3.8956
1024.5771	377.1222	1313.1992	646.2577	1475.1646	47.3409	3107.6624	3.542
1048.7135	0	1314.6346	0	1483.7729	0	3107.6665	0
1049.1174	53.5188	1315.3098	0	1483.7754	12.9222	3218.8779	0
1049.3091	0	1316.0811	913.8702	1484.8417	13.8735	3218.916	24.4439
1049.5686	62.0334	1319.2419	0	1484.9602	0	3221.4097	0
1052.6927	0	1319.7644	924.3799	1486.7303	0	3221.446	20.7949
1053.12	0	1345.8979	0	1486.8969	5.6923	3223.0161	33.62
1053.575	179.892	1346.0634	71.0266	1498.8737	48.683	3223.0215	0
1054.0551	361.5399	1349.5865	0	1499.1572	0	3223.2288	24.2489
1061.5616	0	1350.8397	193.1595	1499.9746	115.5259	3223.2302	0
1062.9187	391.2202	1353.7626	0	1500.0326	0	3224.6284	0
1150.3763	0	1354.9556	76.9966	1506.8451	67.5683	3224.6299	19.9438
1150.3794	4.4718	1364.2341	0	1506.8896	0	3224.7954	28.5898
1162.2494	3.9166	1364.2791	32.2566	1610.8904	60.472	3224.8069	0
1162.2515	0	1367.2747	0	1613.2507	0	3230.7817	0
1166.319	0	1367.5415	41.3065	1615.5862	0	3230.7827	20.5267
1166.3846	1.5789	1369.2303	0	1618.7401	690.5589	3231.4448	27.0212
1240.6893	135.2084	1369.3582	57.0854	1640.0295	0	3231.4531	0
1240.8419	0	1369.6066	0	1645.7317	96.8361	3237.3953	0
1241.6234	46.6453	1369.7725	67.5151	1646.9904	0	3237.4807	113.038
1241.6421	0	1377.9336	0	1653.692	478.6351		
1243.2505	0	1379.5659	200.2331	1666.0964	0		
1243.2968	46.997	1380.469	84.0733	1666.4061	67.5463		
1249.5413	75.4649	1380.4916	0	1672.3979	0		

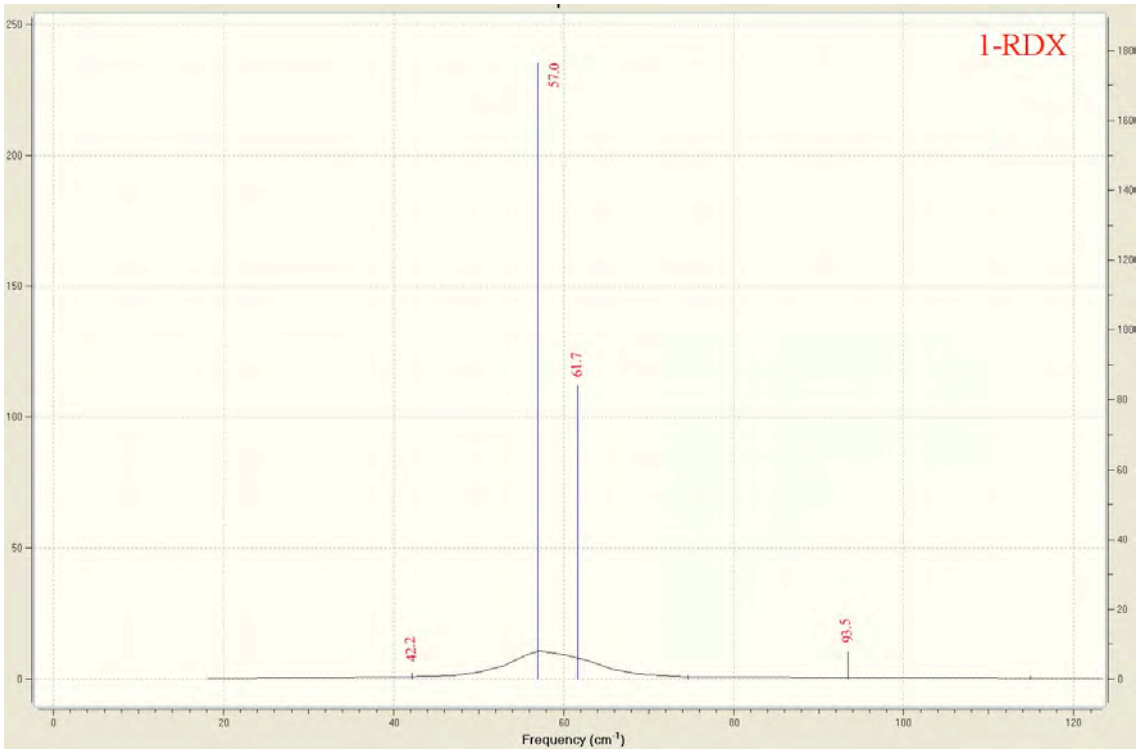

Figure 6. IR intensity as a function of frequency calculated using DFT B3LYP/6-311G(2d,2p) for single isolated molecule of RDX according to frozen phonon approximation.

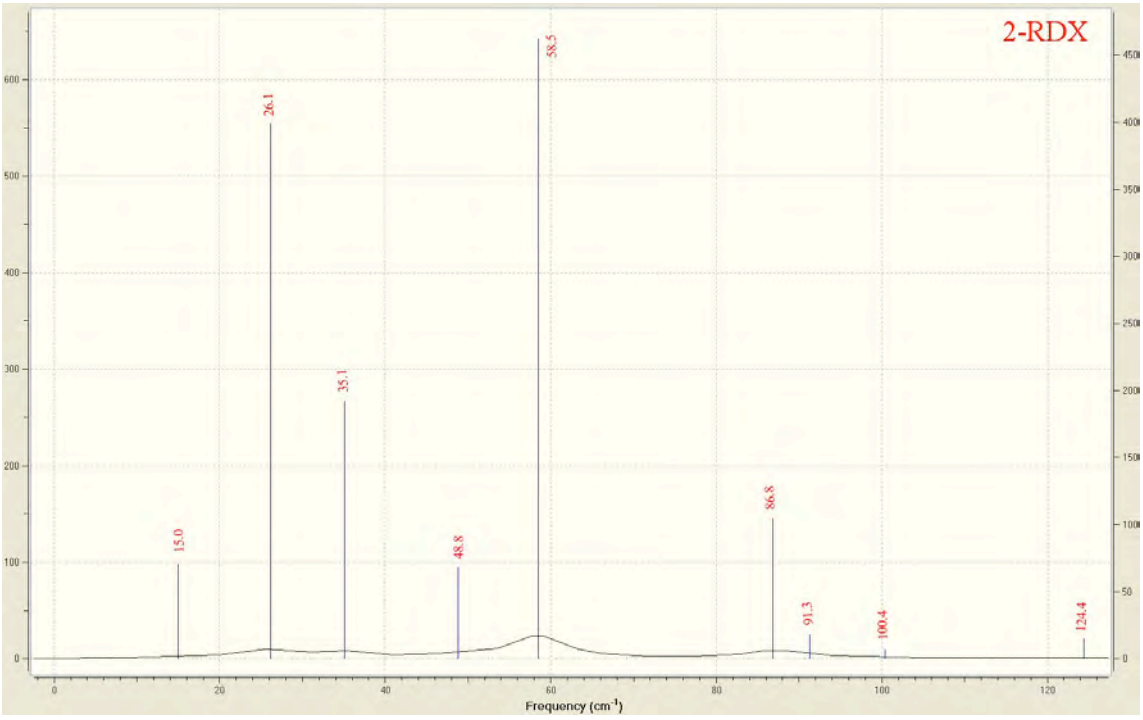

Figure 7. IR intensity as a function of frequency calculated using DFT B3LYP/6-311G(2d,2p) for two-molecule cluster of RDX according to frozen phonon approximation.

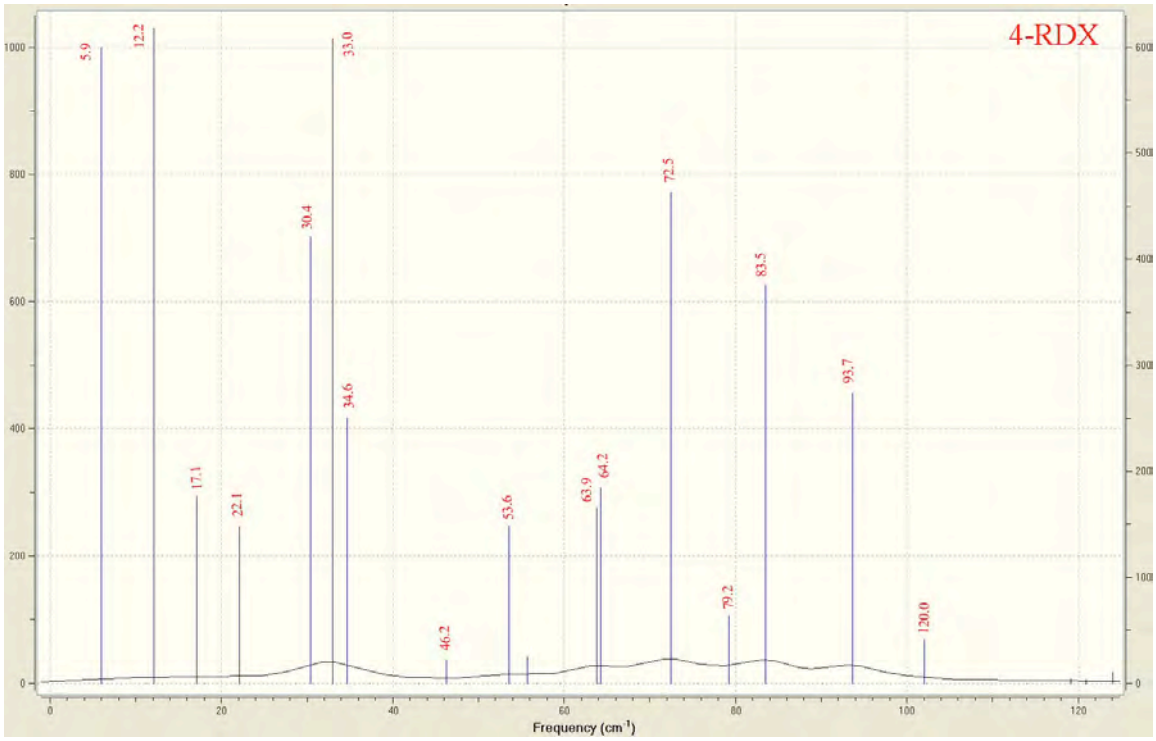

Figure 8. IR intensity as a function of frequency calculated using DFT B3LYP/6-311G(2d,2p) for four-molecule cluster of RDX according to frozen phonon approximation.

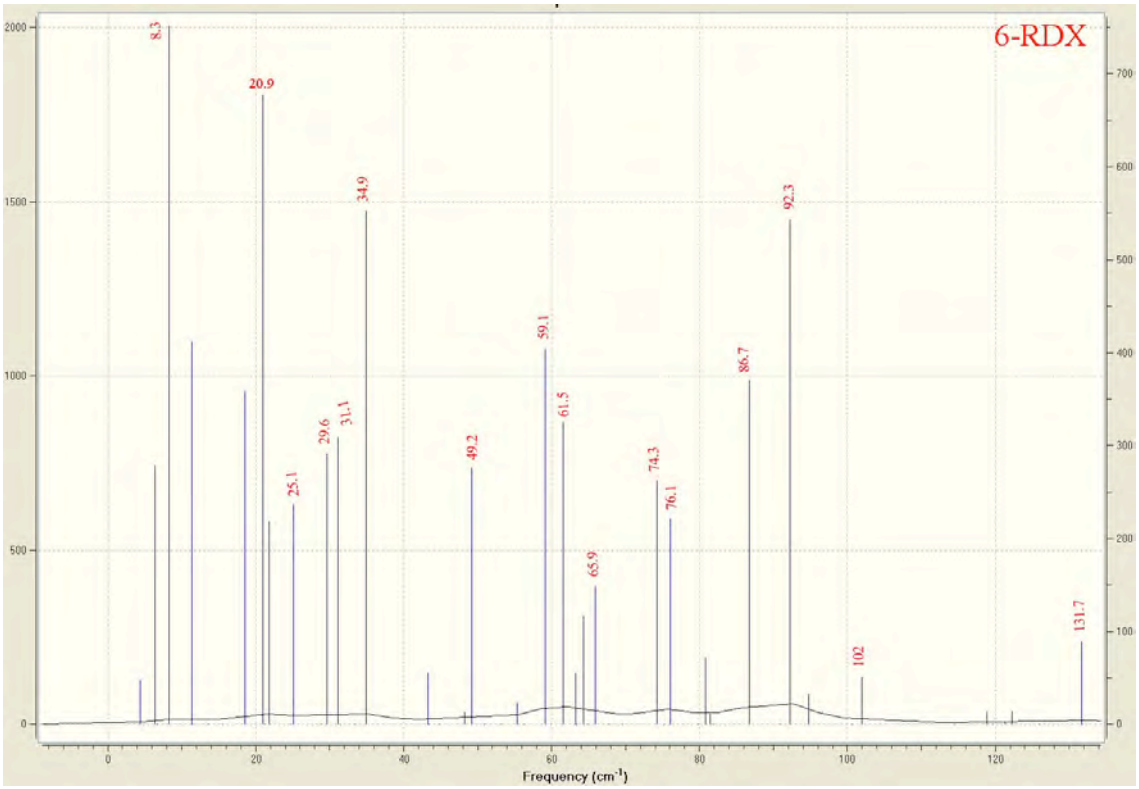

Figure 9. IR intensity as a function of frequency calculated using DFT B3LYP/6-311G(2d,2p) for six-molecule cluster of RDX according to frozen phonon approximation.

Shown in Figs. 10 and 11 are spectra of clusters in comparison with experimentally measured spectra [19, 20]. Referring to these figures, initial consideration is given to what extent various average features of the DFT calculated spectra for different size molecular clusters, as well as experimentally measured spectra, are correlated with each other. Referring to Fig. 10, one observes on average a noticeable correlation between DFT calculated spectra for molecule clusters of RDX and experimentally measured spectrum for dielectric response of RDX solid. The comparison of spectra shown in Fig. 10 also supports the notion that certain resonance features, which are associated with finite-size molecular clusters, are preserved within clusters of increasing size, as well as in solid form, thus implying a persistence of these modes after coupling to intermolecular influences. The persistence of certain intramolecular modes, which is irrespective of molecular cluster size, i.e., whether the molecule is isolated, part of a cluster or within a bulk lattice, is demonstrated by comparison of DFT calculated and experimentally measured spectra. Shown in Shown in Table 6 is a comparison of DFT calculated frequencies corresponding to prominent absorptions, which have been observed experimentally for RDX in solid state. Referring to this table, one can observe a high correlation between DFT calculated spectra for different cluster sizes and experimentally determined absorption lines at the specific frequencies indicated.

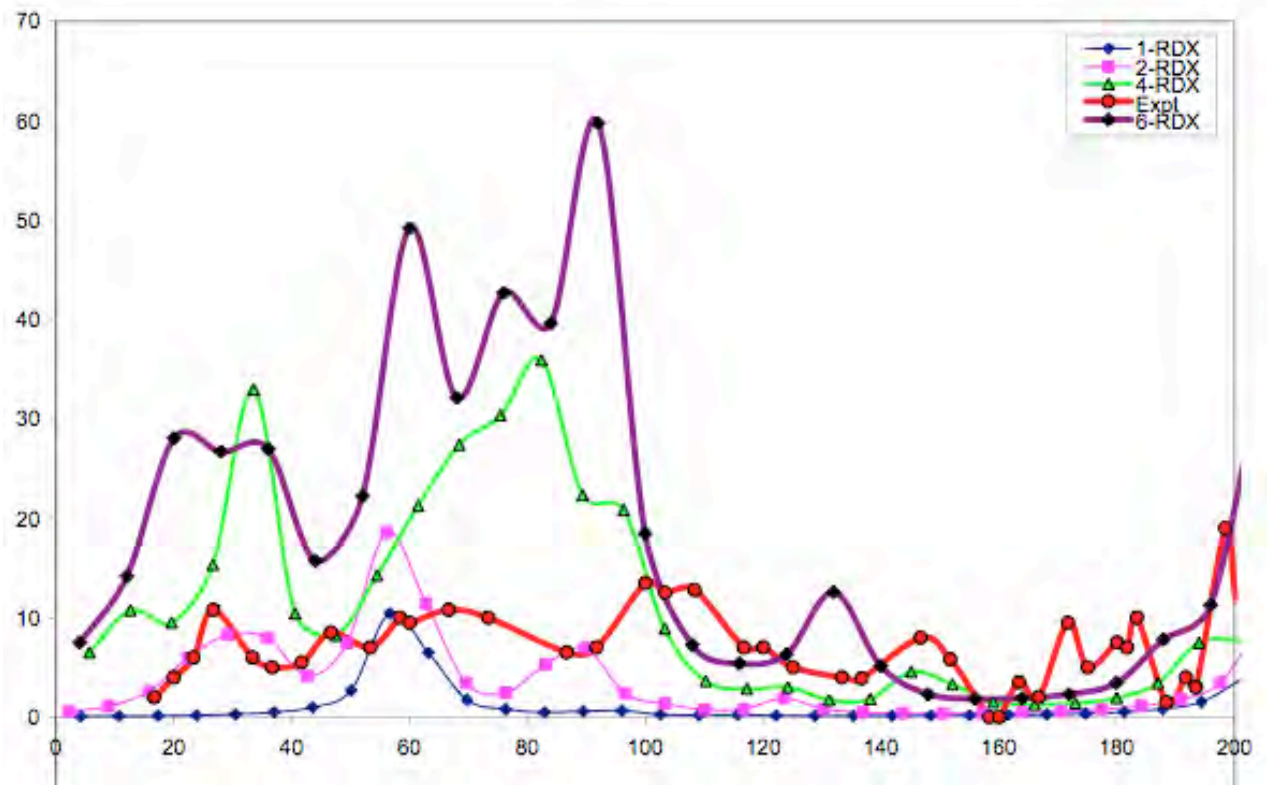

Figure 10. Qualitative comparison of DFT calculated spectra for 1-, 2-, 4- and 6-molecule clusters of RDX and experimentally measured spectrum for dielectric response of RDX solid.

Table 6. Comparison of DFT calculated and experimentally measured frequencies at prominent absorptions for RDX solid [19].

Exp (cm^{-1})	27	35	46	51	66	74	103
1-RDX	-	-	42	57	62	-	94
2-RDX	26	35	49	59	-	87	100
4-RDX	17-22	33	46	54	64	73	84-94
6-RDX	21	35	49	59	66	74	92

Referring to Fig. 11, one observes on average a noticeable correlation between DFT calculated spectra for molecule clusters of RDX and experimentally measured spectrum for dielectric response of RDX vapor. Shown in Shown in Table 7 is a comparison of DFT calculated frequencies corresponding to prominent absorptions, which have been observed experimentally for RDX in vapor state. Referring to this table, one can observe a high correlation between DFT calculated spectra for different cluster sizes and experimentally determined absorption lines at the specific frequencies indicated.

Table 7. Comparison of DFT calculated and experimentally measured frequencies at prominent absorptions for RDX vapor [20].

Exp (cm^{-1})	1272	1602
1-RDX	1310	1663-1701
2-RDX*	1306	1677
4-RDX*	1314	1696
6-RDX*	1316	1673

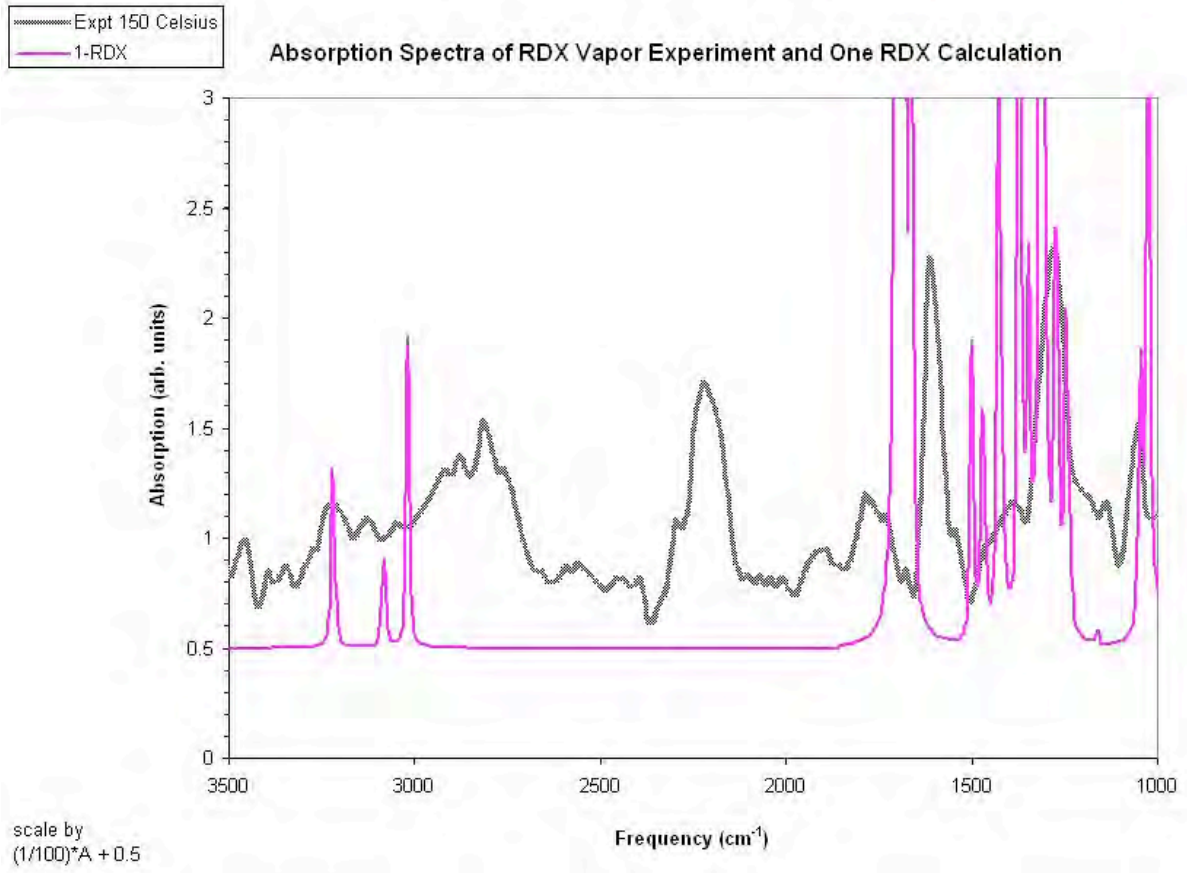

Figure 11(a). Qualitative comparison of DFT calculated spectra for single isolated molecule of RDX and experimentally measured spectrum for dielectric response of RDX vapor.

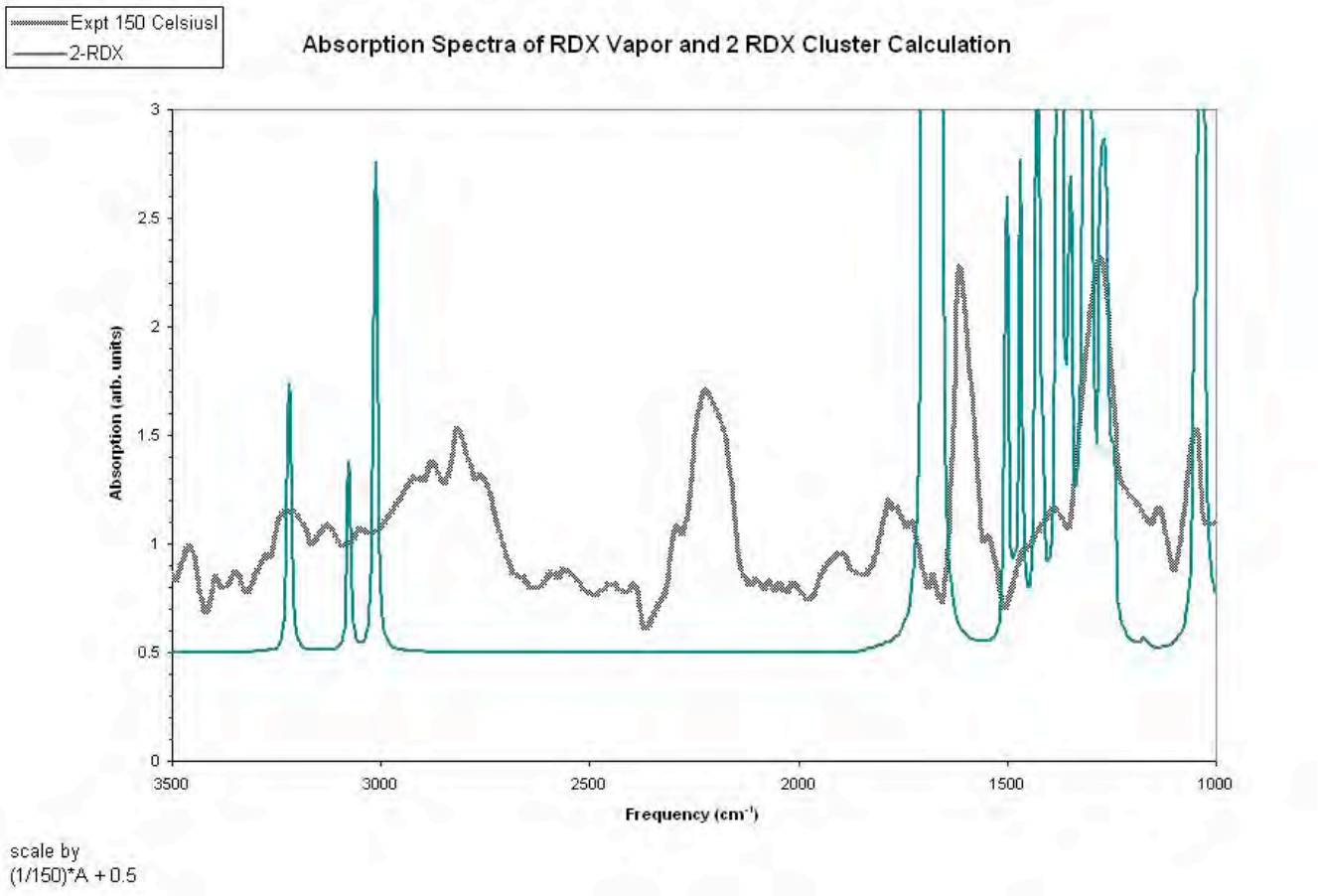

Figure 11(b). Qualitative comparison of DFT calculated spectra for 2-molecule cluster of RDX and experimentally measured spectrum for dielectric response of RDX vapor.

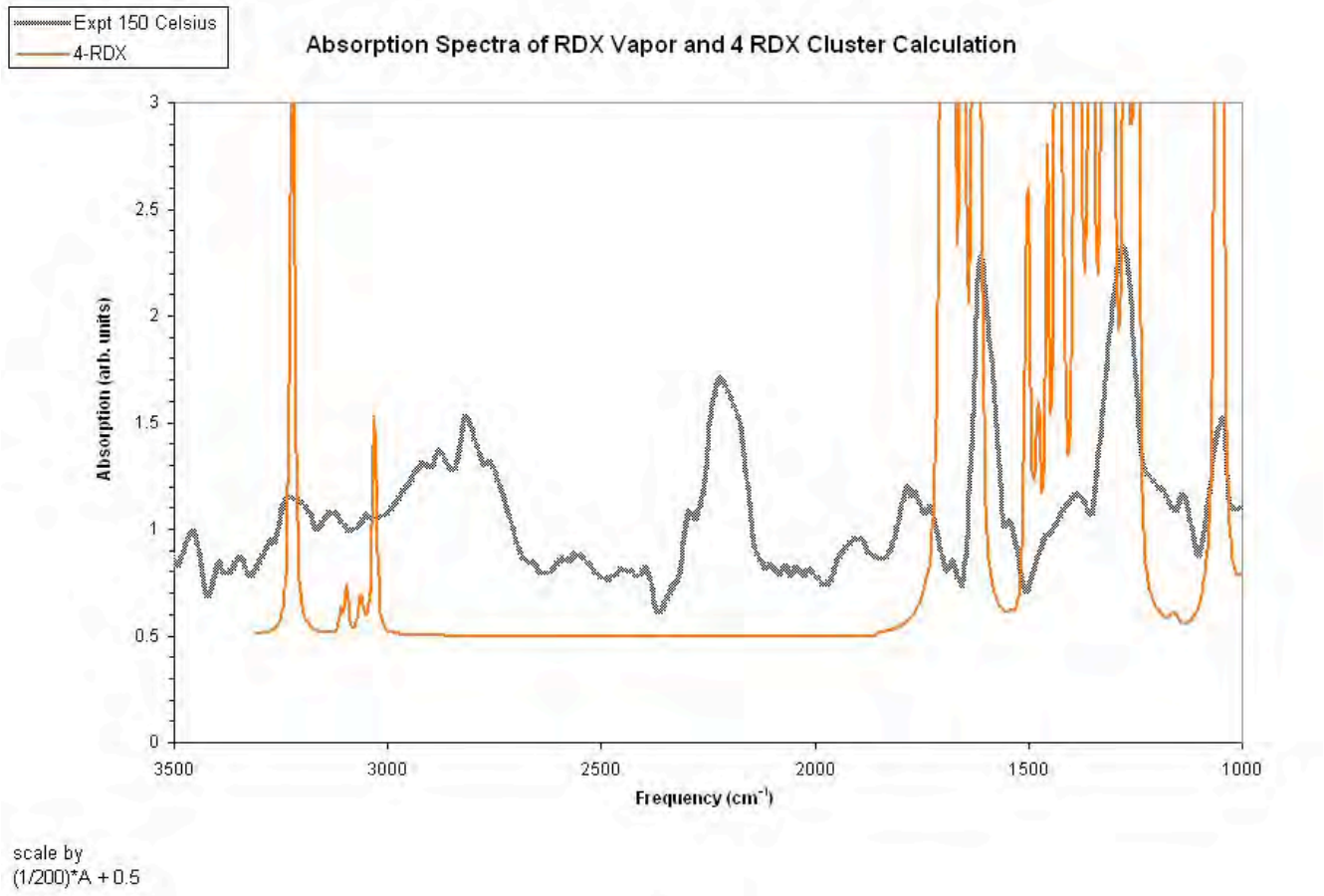

Figure 11(c). Qualitative comparison of DFT calculated spectra for 4-molecule cluster of RDX and experimentally measured spectrum for dielectric response of RDX vapor.

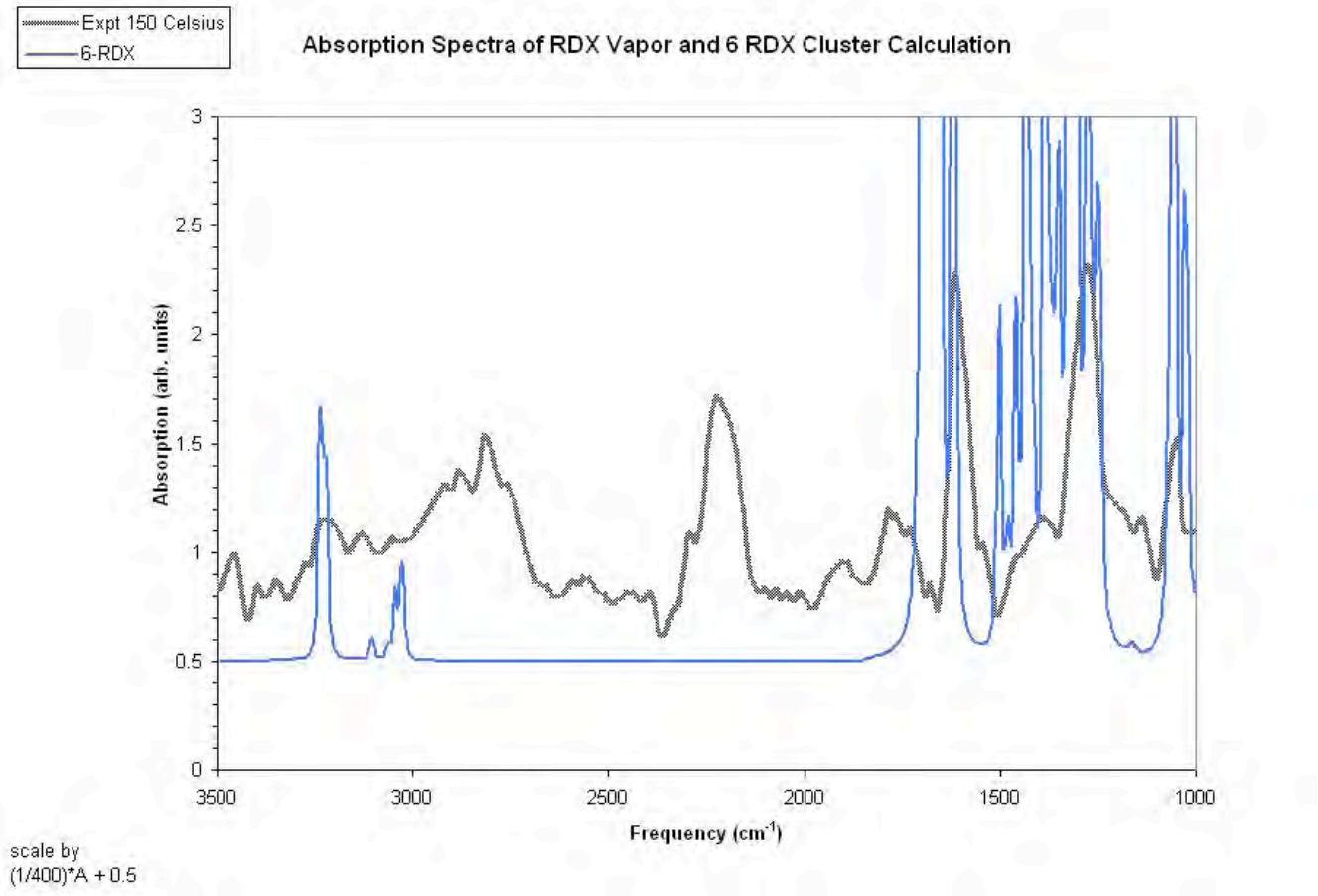

Figure 11(d). Qualitative comparison of DFT calculated spectra for 6-molecule cluster of RDX and experimentally measured spectrum for dielectric response of RDX vapor.

Ground State Resonance Structure of 3-Molecule Cluster of PETN

In this section are presented the results of computational experiments using DFT concerning 3-molecule cluster of PETN. These results include the relaxed or equilibrium configuration of a single isolated molecule of PETN (see Table 8) and ground-state oscillation frequencies and IR intensities for this configuration, which are calculated by DFT according to the frozen phonon approximation (see Table 9). The ground state resonance structure for a single isolated molecule of PETN is adopted as a reference for analysis of spectral features associated with a 3-molecule cluster. For these calculations geometry optimization and vibrational analysis was effected using the DFT model B3LYP [12, 13] and basis function 6-311G(2d,2p) [14,15]. According to the specification of this basis function, (2d,2p) designates polarization functions having 2 sets of d functions for heavy atoms and 2 sets of p functions for hydrogen atoms [16]. A schematic representation of the molecular geometry of a single isolated molecule of PETN is shown in Fig.(12). A schematic representation of the molecular geometry of a molecular cluster consisting of 3 molecules is shown in Figs. (13). It is significant to note that the relative positions of the molecules associated with this molecular cluster are according to crystallographic structure conditions that would be associated with bulk material. In particular, the crystal structure of PETN, whose CCDC reference code is PEYTN01, has been investigated by H. H. Cady, A. C. Larson (1975) [21]. The space group for this crystal structure is ***P****cnb* (symmetry operators are x, y, z; ½-x, y, ½+z; ½+x, ½-y, ½+z; -x, ½-y, z; -x, -y, -z; ½+x, -y, ½-z; ½-x, ½+y, ½-z; x, ½+y, -z), and the unit cell constants are a=13.290, b=13.490, c=6.830, α=90.00, β=90.00, γ=90.00 and density 1.715 g/cm^3. The ground-state oscillation frequencies and IR intensities for the 3-molecule cluster of PETN, corresponding to its relaxed equilibrium configuration, are calculated by DFT according to the frozen phonon approximation. In the case of a molecular cluster of 3 molecules, these values are given in Table 10. The DFT model and basis function used for these calculations are the same as those used for the single isolated molecule of PETN.

Table 8. Atomic positions of PETN (Å) after optimization.

Atomic number	X	Y	Z	Atomic number	X	Y	Z
6	-0.89008	0.487044	0.169443	8	1.885603	-3.148164	-0.06536
6	0.56833	0.025631	0.355901	8	2.801652	-1.246607	0.487954
6	-0.954153	2.010353	0.393203	1	-1.969444	2.373078	0.253141
6	-1.775405	-0.266852	1.180709	1	-0.289344	2.531375	-0.29121
6	-1.399001	0.17896	-1.25209	1	0.903906	0.201954	1.374781
8	-0.536524	2.246621	1.753563	1	1.224466	0.550575	-0.333979
8	0.594489	-1.388358	0.071682	1	-1.43301	-0.084138	2.196278
8	-3.114945	0.243543	1.019535	1	-1.763653	-1.336176	0.985073
8	-0.503707	0.845656	-2.165744	1	-2.410743	0.55161	-1.391197
8	-5.169236	0.102355	1.756224	1	-1.382201	-0.89204	-1.438315
8	-3.660475	-1.176108	2.678384	7	-4.069163	-0.341502	1.911776
8	-0.213539	3.790051	3.268901	7	-0.561634	3.625752	2.13612
8	-0.916392	4.418249	1.301021	7	1.895046	-1.976796	0.177844
8	-0.065066	1.202636	-4.278301	7	-0.825239	0.640236	-3.54537
8	-1.784867	-0.046988	-3.786458				

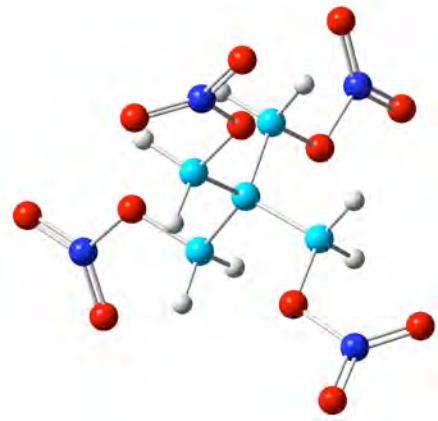

Figure 12. Molecular Geometry of PETN

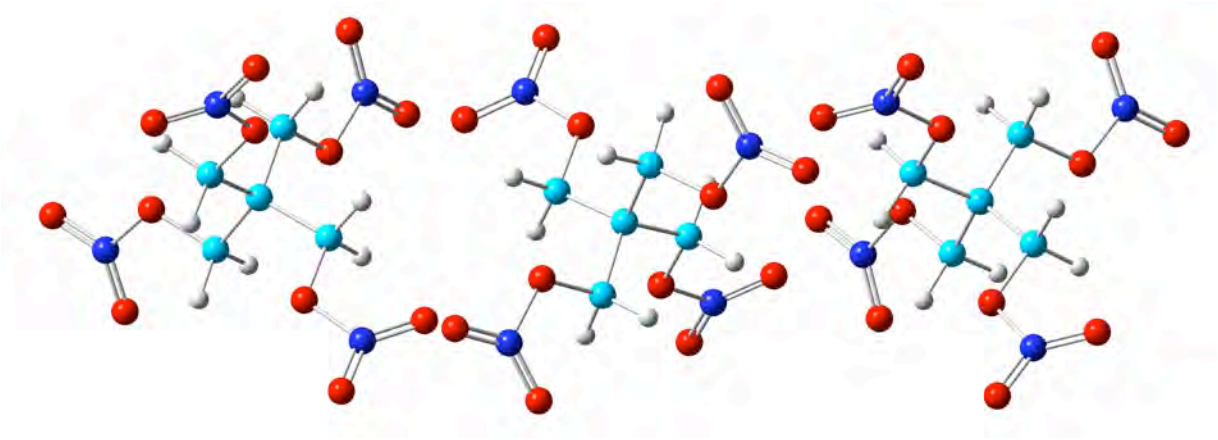

Figure 13. Molecular Geometry of 3-Moleculae Cluster of PETN

Proceeding, shown in Figs. 14 and 15 are calculated IR intensities for a single isolated molecule and 3-molecule cluster of PETN. Shown in Figs. 16 and 17, are continuous spectra consisting of a superposition of essentially Lorenzian functions of various heights and widths, which have been constructed using the discrete spectra given in Tables 9 and 10, respectively.

Table 9. Oscillation frequencies and IR intensities for single isolated molecule of PETN.

Frequency cm^{-1}	Intensity (km/mol)	Frequency cm^{-1}	Intensity (km/mol)	Frequency cm^{-1}	Intensity (km/mol)	Frequency cm^{-1}	Intensity (km/mol)
23.0186	0	319.7365	0	927.126	12.2082	1410.9192	64.19
23.468	1.7622	453.5805	3.6627	944.6012	7.5925	1425.4355	0
37.0668	0.0792	453.5809	3.6627	944.6018	7.5925	1513.7205	0
38.2553	1.0181	533.9816	12.509	1015.2359	0	1514.457	4.0158
38.256	1.0182	589.553	0	1031.1128	68.9949	1520.2629	13.4384
49.1445	0	620.4669	9.0561	1031.1133	68.9954	1520.2631	13.4385
51.2098	0.0198	625.7476	8.654	1063.903	0	1765.1326	0
56.1273	1.4445	625.7479	8.6542	1069.3729	100.3831	1766.3812	231.1996
56.1281	1.4444	676.3956	0	1184.1914	2.4068	1767.5533	544.1035
125.0831	0.5041	711.7268	53.505	1203.243	0.1994	1767.554	544.1009
125.0838	0.5041	711.7271	53.5047	1203.2433	0.1994	3081.5559	5.7489
137.2362	0.8057	756.1322	54.9232	1264.3964	0	3082.5044	7.1942
149.3	0	775.0616	12.1352	1284.5981	21.2105	3082.5051	7.1942
175.381	0	775.0623	12.1353	1284.5988	21.2112	3084.4409	0
198.2257	0.822	775.6437	0	1310.0272	243.6025	3139.0088	0
198.2262	0.822	776.5314	30.3068	1329.7418	272.2731	3140.7324	5.4891
213.1381	0	842.7866	0	1329.7419	272.2725	3140.7327	5.4894
253.3021	2.0613	857.2537	365.5689	1343.2953	0	3143.0876	10.9428
256.0704	1.9542	857.2545	365.5689	1344.2228	196.2847		
256.0709	1.9542	861.1535	708.764	1406.7094	43.0983		
309.178	1.5099	887.0866	0	1406.7097	43.0982		

Table 10. Oscillation frequencies and IR intensities for 3-molecule cluster of PETN.

Frequency cm^{-1}	Intensity (km/mol)	Frequency cm^{-1}	Intensity (km/mol)	Frequency cm^{-1}	Intensity (km/mol)	Frequency cm^{-1}	Intensity (km/mol)
2.7459	0.005	143.6774	0.09	625.2445	1.4605	939.29	0.062
3.0959	0	150.8196	0	625.2576	16.8618	942.0798	0.9418
5.9927	0	151.0548	0.6581	630.3136	20.158	942.9281	15.3538
9.3696	0.0003	151.6617	0	630.4765	2.2566	948.6176	15.6586
9.4769	0.0102	179.9747	0.0565	633.2105	21.9922	948.6245	2.9713
12.6516	0.0555	179.9893	0.091	677.9521	2.6767	950.0091	9.2565
19.0972	0.6809	187.9166	0.0943	677.9772	0.5639	1013.7078	0.5689
21.5863	0.0499	191.0116	1.1948	679.5992	1.3293	1014.4844	1.6776
23.4909	3.1816	193.9818	4.2534	711.3558	37.4622	1014.6168	1.0282
24.2182	0.0223	193.9882	0.0045	711.5214	0.0131	1021.6065	38.8561
24.2957	0.1038	203.0462	1.4143	711.6724	135.8772	1026.3538	0.189
26.1885	0.0298	203.1005	0.0342	714.8454	67.0988	1026.4937	140.2393
27.792	0.0928	204.4253	0.2964	714.9153	4.0388	1033.9843	152.6453
29.53	0.6686	215.1988	0.0063	717.5967	55.4965	1034.1356	0.5469
32.3744	0.148	215.2201	0.0489	754.8807	8.6665	1036.3997	108.9989
33.728	0.6131	216.7523	0.0112	755.7139	6.5923	1060.5533	11.1806
36.5112	0.1353	253.5204	2.5784	755.9681	125.2554	1063.3865	1.689
37.9722	1.142	253.5395	1.3166	771.4876	35.9297	1063.7787	52.3445
40.1106	0.1238	255.4469	2.9787	771.5766	0.5576	1068.8099	46.4614
40.2686	0.7434	256.9556	4.6241	772.0193	52.9692	1069.15	1.7564
40.6739	0.0067	256.9622	0.0114	772.045	32.2983	1070.5229	152.8388
41.148	0.0902	258.4687	2.3891	775.0159	0.3922	1182.1937	0.5315
45.3709	0.8009	260.5664	0.4464	775.0287	17.1464	1183.4821	0.5997
45.4139	0.0058	260.6916	6.0475	775.3692	5.8581	1183.5236	3.8764
49.0572	0.1161	261.354	4.6746	775.3761	7.2323	1200.4976	0.5446
52.0377	0.0004	308.4312	0.5996	775.5979	15.9024	1201.5612	1.1979
52.0415	2.3979	310.0498	1.3298	776.2775	20.1457	1201.5688	0.0735
52.8558	0.211	310.2897	5.5818	776.3102	0.0334	1203.6359	0.3577
54.4623	4.7351	318.7477	0.0604	776.7685	18.1673	1203.7332	0.0599
56.9478	1.8936	319.4577	0.5603	843.0367	11.9947	1203.8767	0.012
56.9559	0.0156	319.48	0.2014	843.3959	10.8952	1264.6515	0.0131
58.1967	0.8009	452.9283	7.3557	844.2677	3.2431	1264.6724	1.2153
59.0884	0.0242	452.9482	0.3582	852.5711	74.5096	1264.6882	0
60.7896	0.0144	454.1579	3.0692	854.7542	1.2119	1284.3719	71.0302
62.0465	2.6393	456.9975	9.8235	855.0319	1113.0496	1284.4592	0.0881
64.1165	0.017	457.2185	0.0887	859.1821	440.0582	1284.9974	15.2172
67.5021	2.5334	458.9726	1.6145	859.2446	328.521	1287.3538	49.0979
81.1563	0.063	535.0382	21.8539	862.1922	204.4109	1287.3636	0.2869
82.4234	0.2897	535.0643	0.3361	867.808	188.3015	1289.071	24.2026
123.768	1.6121	536.2878	2.4334	870.1517	767.9538	1308.4966	10.5086
123.9862	0.0784	590.701	0.0464	872.9782	442.748	1310.3143	22.3865
125.3659	0.059	590.7104	0.044	890.1616	10.2077	1312.6071	576.5331
129.7586	0.995	591.5033	0.0049	891.835	78.6084	1324.9568	463.472
129.8118	0.2058	621.6932	9.3787	896.2267	265.5877	1326.1389	650.3981
140.6045	1.3884	621.7182	2.4644	928.7986	20.8334	1328.1746	0.0026
140.8086	0.7455	623.7837	6.7643	928.7987	0.2006	1330.5981	0.0236
141.5511	0.6157	624.7261	0.1423	931.284	22.9396	1331.6897	357.7667

Table 10 (continued)

Frequency cm^{-1}	Intensity (km/mol)	Frequency cm^{-1}	Intensity (km/mol)	Frequency cm^{-1}	Intensity (km/mol)	Frequency cm^{-1}	Intensity (km/mol)
1332.6163	325.2102	1426.7509	1.5948	1753.121	121.7147	3095.5657	10.7196
1341.1545	0.0623	1427.8077	0.8237	1766.1827	656.7066	3096.1804	2.0796
1342.6538	0.8549	1504.132	2.0613	1766.2982	0.0164	3098.1538	3.8464
1343.0424	2.8398	1506.4666	40.4544	1766.9027	527.3882	3098.1646	1.7708
1344.1932	3.4047	1508.4739	0.522	1767.3317	131.9252	3136.0608	5.0163
1344.3925	9.4586	1511.4553	16.212	1768.5984	63.6771	3136.0637	3.8842
1344.9041	489.2351	1512.9001	0.4156	1769.1071	244.2138	3140.5251	5.7739
1407.7294	75.5986	1513.5698	2.3789	1770.5093	937.002	3140.7388	9.6767
1407.7589	0.0147	1513.6084	1.62	1770.6707	151.094	3140.7444	0.0509
1408.5706	80.8585	1516.7607	3.007	3078.3787	9.9733	3140.7461	5.9203
1408.7397	11.8525	1516.7999	16.3591	3078.3806	3.0626	3147.1145	6.1931
1408.9039	56.6913	1518.0491	10.1118	3079.4727	12.1956	3147.1213	5.1318
1410.5243	34.4459	1519.4949	21.3927	3079.8242	1.1214	3155.8755	4.9167
1412.4119	12.556	1519.5026	0.0019	3081.5474	8.191	3156.3723	4.0165
1412.4762	67.0457	1746.3506	1019.5118	3081.5496	2.1684	3160.1804	3.5558
1413.4799	85.1998	1746.6143	236.3832	3083.6433	13.4875	3160.1809	5.7426
1426.6968	0.2855	1752.1338	0.2487	3083.6489	0.0252		

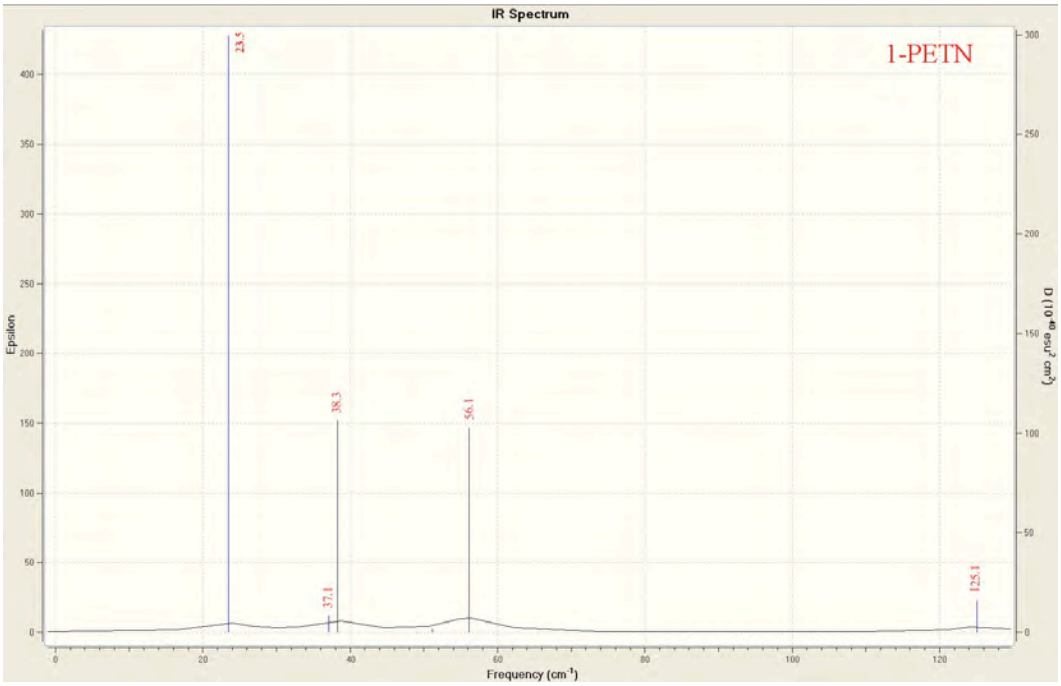

Figure 14. IR intensity as a function of frequency calculated using DFT B3LYP/6-311G(2d,2p) for single isolated molecule of PETN according to frozen phonon approximation.

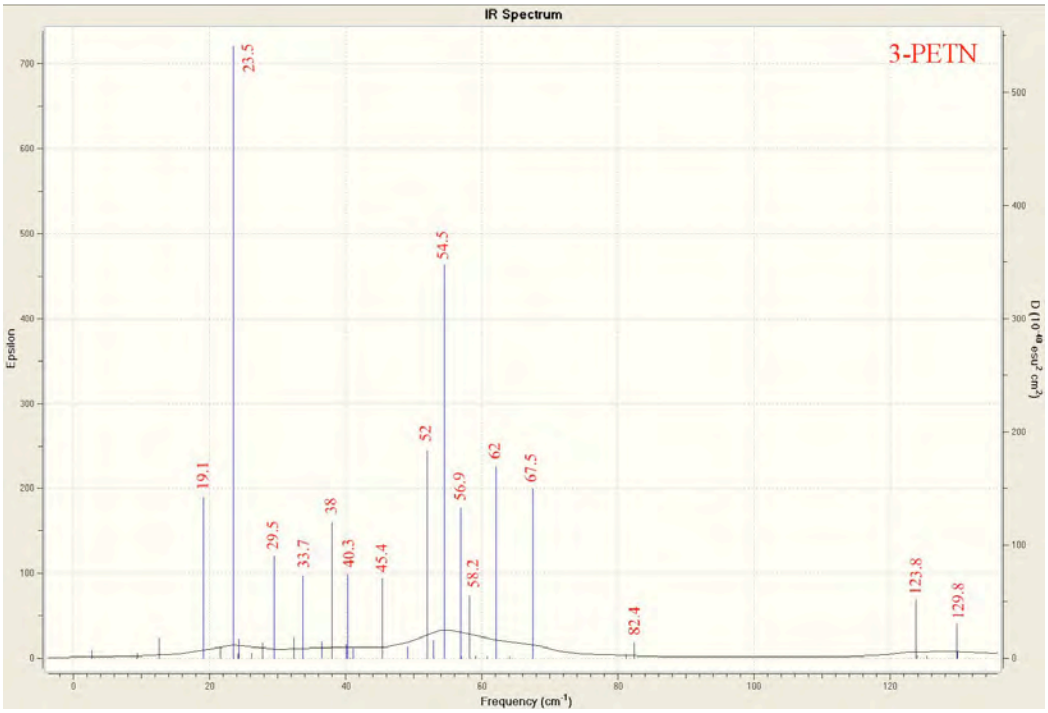

Figure 15. IR intensity as a function of frequency calculated using DFT B3LYP/6-311G(2d,2p) for three-molecule cluster of PETN according to frozen phonon approximation.

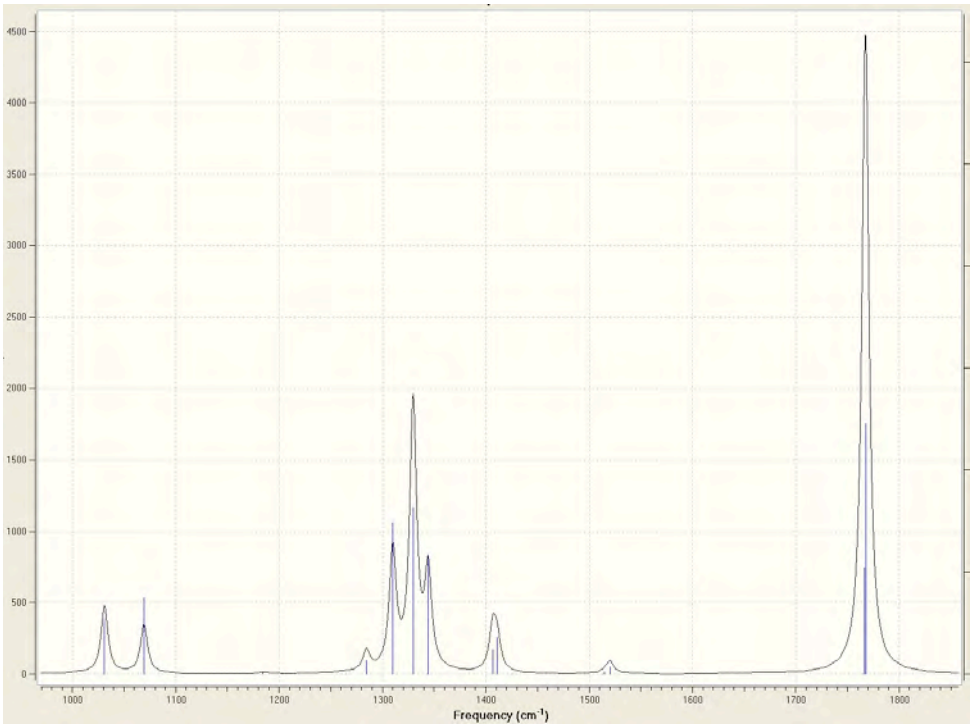

Figure 16. Continuous-spectrum representation of IR intensity as a function of frequency calculated using DFT for single isolated molecule of PETN.

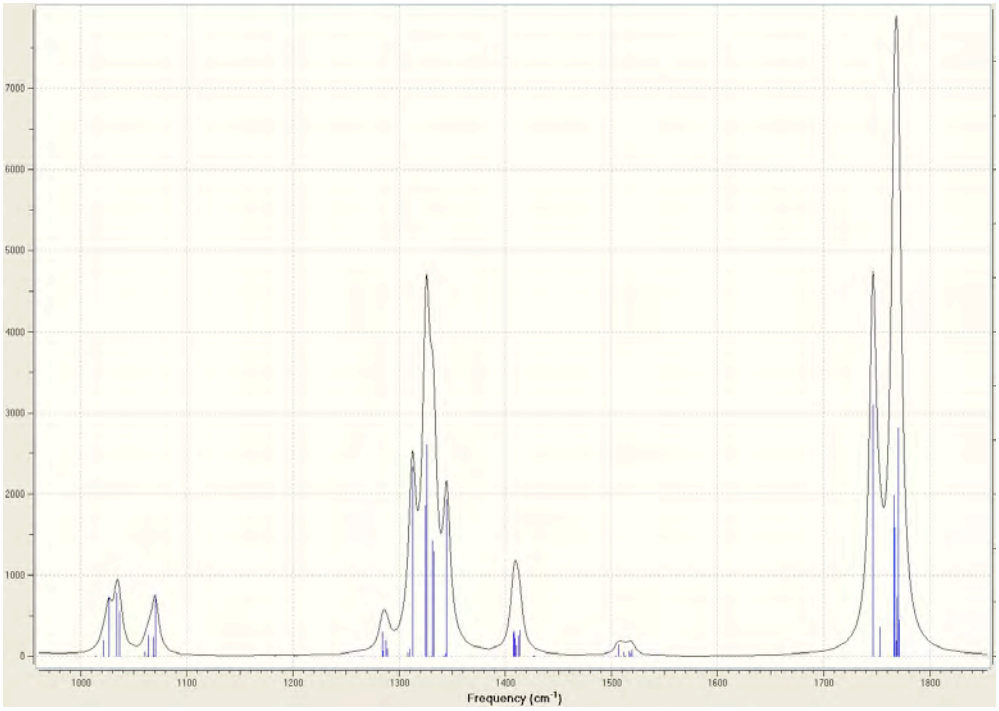

Figure 17. Continuous-spectrum representation of IR intensity as a function of frequency calculated using DFT for three-molecule cluster of PETN.

Shown in Figs. 18 and 19 are spectra of clusters in comparison with experimentally measured spectra [19, 20]. Referring to these figures, initial consideration is given to what extent various average features of the DFT calculated spectra for different size molecular clusters, as well as experimentally measured spectra, are correlated with each other. Referring to Fig. 18, one observes on average a noticeable correlation between DFT calculated spectra for molecule clusters of PETN and experimentally measured spectra for the dielectric response of PETN solid. The comparison of spectra shown in Fig. 18 also supports the notion that certain resonance features, which are associated with finite-size molecular clusters, are preserved within clusters of increasing size, as well as in solid form, thus implying a persistence of these modes after coupling to intermolecular influences. The persistence of certain intramolecular modes, which is irrespective of molecular cluster size, i.e., whether the molecule is isolated, part of a cluster or within a bulk lattice, is demonstrated by comparison of DFT calculated and experimentally measured spectra. Shown in Table 11 is a comparison of DFT calculated frequencies corresponding to prominent absorptions, which have been observed experimentally for PETN in solid state. Referring to this table, one can observe a high correlation between DFT calculated spectra for different cluster sizes and experimentally determined absorption lines at the specific frequencies indicated.

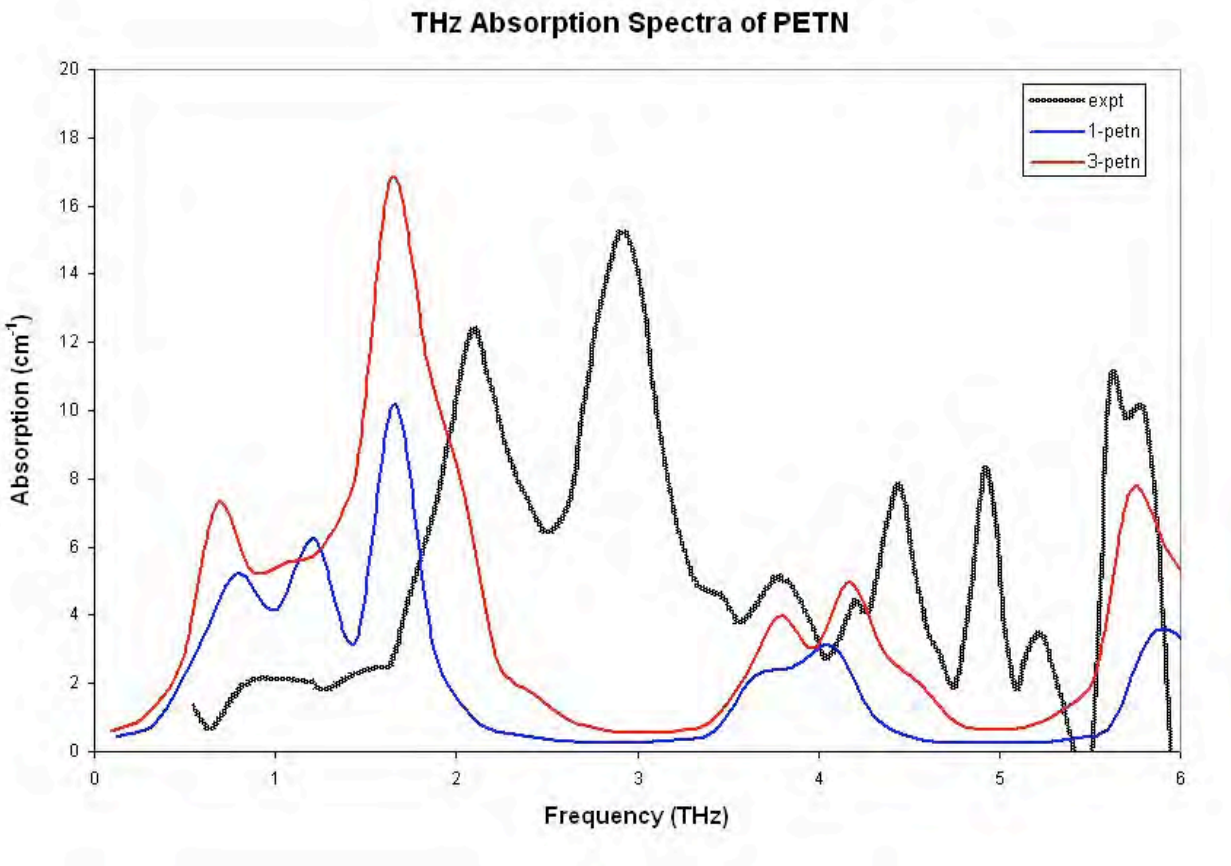

Figure 18. Qualitative comparison of DFT calculated spectra for 1-and 3-molecule clusters of PETN and experimentally measured spectrum for dielectric response of PETN solid.

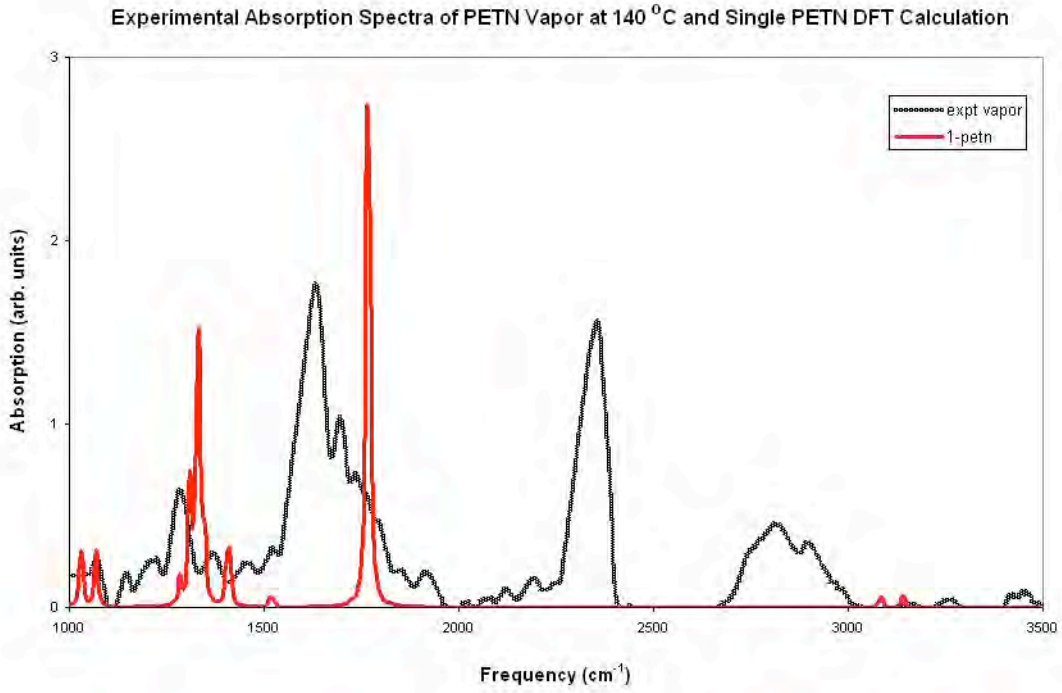

Figure 19(a). Qualitative comparison of DFT calculated spectra for single PETN and experimentally measured spectrum for dielectric response of PETN vapor.

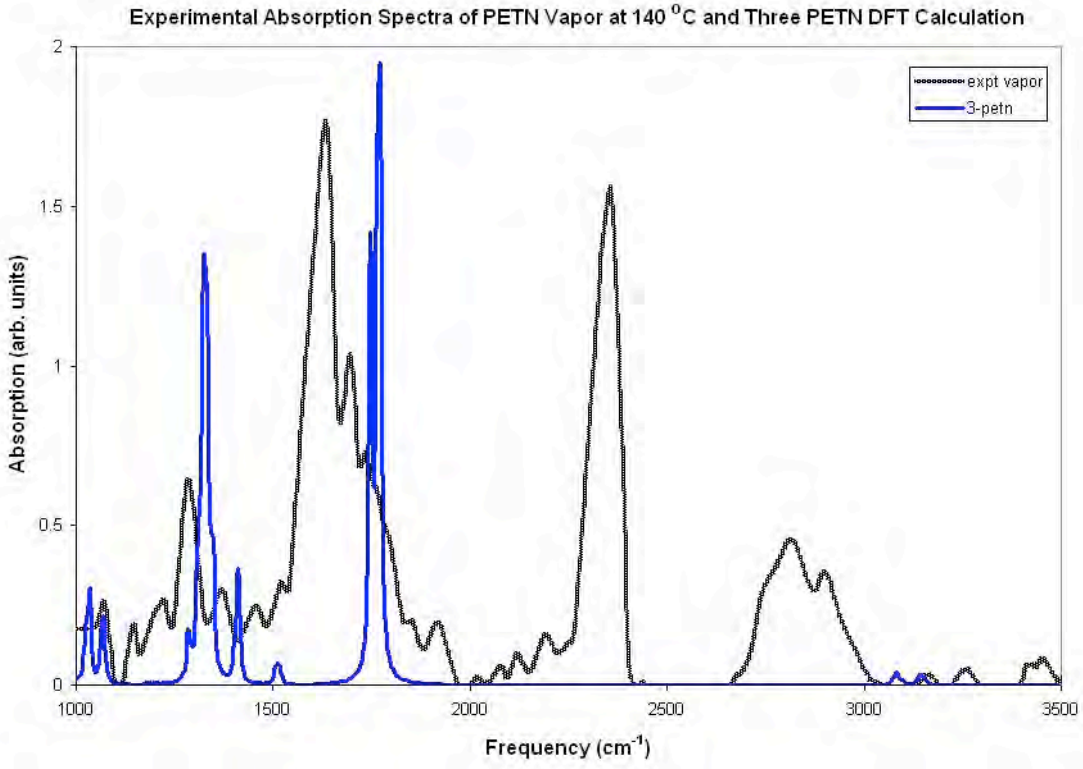

Figure 19(b). Qualitative comparison of DFT calculated spectra for three PETN and experimentally measured spectrum for dielectric response of PETN vapor.

Table 11. Comparison of DFT calculated and experimentally measured frequencies at prominent absorptions for PETN solid [19].

Expt(cm^{-1})	67	72	96
1-PETN	56	-	(125)
3-PETN	54-68	82	(124)

Referring to Figs. 19, one observes on average a noticeable correlation between DFT calculated spectra for molecule clusters of PETN and experimentally measured spectrum for dielectric response of PETN vapor. Shown in Table 12 is a comparison of DFT calculated frequencies corresponding to prominent absorptions, which have been observed experimentally for PETN in vapor state. Referring to this table, one can observe a high correlation between DFT calculated spectra for different cluster sizes and experimentally determined absorption lines at the specific frequencies indicated.

Table 12. Comparison of DFT calculated and experimentally measured frequencies at prominent absorptions for PETN vapor [20].

Expt(cm^{-1})	1279	1626
1-PETN	1329	1768
3-PETN*	1326	1746

Ground State Resonance Structure of Molecular Clusters of TNT

In this section are presented the results of computational experiments using DFT concerning molecular clusters of TNT. These results include the relaxed or equilibrium configuration of a single isolated molecule of TNT (see Table 13) and ground-state oscillation frequencies and IR intensities for this configuration, which are calculated by DFT according to the frozen phonon approximation (see Table 14). The ground state resonance structure for a single isolated molecule of TNT is adopted as a reference for analysis of spectral features associated with molecular clusters of different sizes. For these calculations geometry optimization and vibrational analysis was effected using the DFT model B3LYP [12, 13] and basis function 6-311G(2d,2p) [14,15]. According to the specification of this basis function, (2d,2p) designates polarization functions having 2 sets of d functions for heavy atoms and 2 sets of p functions for hydrogen atoms [16]. A schematic representation of the molecular geometry of a single isolated molecule of TNT is shown in Fig. 20. A schematic representation of molecular geometries of molecular clusters consisting of 2 and 4 molecules are shown in Figs. 21 and 22, respectively. It is significant to note that the relative positions of the molecules associated with each of the molecular clusters is according to crystallographic structure conditions that would be associated with bulk material. In particular, the crystal structure of TNT, whose CCDC reference code is ZZZMUC05, has been investigated by N. I. Golovina, A. N. Raevskii, L. O. Atovmyan (1994) [22]. The space group for this crystal structure is ***P21ab*** (symmetry operators are x, y, z; x, ½+y, -z; ½+x, -y, -z; ½+x, ½-y, z), and the unit cell constants are a=20.041, b=15.013, c=6.084, α=90.00, β=90.00, γ=90.00 and density 1.648 g/cm^3. The ground-state oscillation frequencies and IR intensities for the different molecular clusters of TNT, corresponding to their relaxed equilibrium configurations, are calculated by DFT according to the frozen phonon approximation. In the cases of molecular clusters of 2 and 4 molecules, these values are given in Tables 15 and 16, respectively. The DFT model and basis function used for these calculations are the same as those used for the single isolated molecule of TNT.

Table 13. Atomic positions for equilibrium configuration of TNT (Å)

Atomic number	X	Y	Z	Atomic number	X	Y	Z
1	1.294359	-0.627693	1.916458	6	1.399735	-0.432944	-2.779328
1	-2.458208	-0.867791	-0.128619	7	-1.347001	-0.883583	2.313715
1	0.754635	0.052629	-3.504585	7	2.841751	-0.500544	-0.177322
1	1.68668	-1.400164	-3.189867	7	-1.547799	-0.781608	-2.569596
1	2.304987	0.153675	-2.659394	8	3.474661	-1.155138	-0.992685
6	0.730091	-0.664364	0.998736	8	3.321537	0.203741	0.698298
6	-0.646569	-0.782893	1.016672	8	-0.658543	-0.86075	3.323182
6	-1.382696	-0.799534	-0.152696	8	-2.564711	-0.982781	2.284321
6	-0.701136	-0.724375	-1.355556	8	-2.607727	-0.174823	-2.533999
6	0.693755	-0.609698	-1.463028	8	-1.14092	-1.451907	-3.507164
6	1.364308	-0.592195	-0.229936				

Table 14. Oscillation frequencies and IR intensities for single isolated molecule of TNT.

Frequency cm^{-1}	Intensity (km/mol)	Frequency cm^{-1}	Intensity (km/mol)	Frequency cm^{-1}	Intensity (km/mol)	Frequency cm^{-1}	Intensity (km/mol)
48.1344	0.1511	470.7113	1.3672	960.2885	2.6521	1479.3087	11.0602
54.4696	0.0031	481.9805	0.0293	966.588	10.2579	1495.7421	9.6734
54.6314	0.449	541.3526	1.0016	1046.3734	3.8264	1608.9564	75.6162
95.2736	4.9386	548.7636	2.1862	1051.7325	1.107	1626.0082	155.939
120.4472	4.6364	662.2958	9.245	1093.3557	53.251	1637.3636	7.7795
149.4345	2.5947	667.0623	0.0724	1183.9727	9.8852	1668.2966	226.3714
176.8858	0.2872	717.9113	20.7181	1208.2366	14.9414	1668.9285	185.4888
187.9397	0.1349	739.4252	51.7192	1220.3445	0.256	3075.5823	0.8369
195.623	4.7398	760.6036	27.3511	1354.5992	4.7978	3143.8171	5.2936
296.0832	1.9743	790.626	0.2088	1389.0625	326.8959	3175.73	4.0642
324.2345	0.2144	797.0792	6.7309	1392.5596	309.3893	3256.9297	12.3643
327.7225	0.0382	805.7737	11.3147	1402.1146	5.7057	3257.0266	29.788
352.9275	2.4697	843.4395	1.7202	1422.838	4.377		
367.8506	1.3391	919.629	37.1859	1423.0629	6.7083		
386.8114	1.1556	951.7191	31.8976	1475.6511	2.6229		

Table 15. Oscillation frequencies and IR intensities for 2-molecule cluster of TNT.

Frequency cm^{-1}	Intensity (km/mol)	Frequency cm^{-1}	Intensity (km/mol)	Frequency cm^{-1}	Intensity (km/mol)	Frequency cm^{-1}	Intensity (km/mol)
8.1269	0.0355	352.9561	1.8829	843.0377	0.4042	1421.4177	9.6829
9.2439	0.1381	353.7762	2.7653	844.2998	3.981	1422.4552	5.9836
14.9722	0.1304	367.1677	1.2469	921.465	5.1014	1424.182	3.6857
17.9857	0.0806	368.4943	1.7859	922.0174	62.7738	1424.5634	7.0426
27.8664	0.1452	385.1874	1.5395	952.5892	34.8719	1475.9287	9.638
51.3591	0.1152	387.5417	1.2049	953.1544	30.8313	1476.429	0.6661
52.1877	0.1647	470.4774	0.6591	959.6472	4.1415	1477.5623	5.8383
54.9708	0.1831	471.4932	1.4576	960.2688	2.7507	1480.2882	9.2747
56.1668	0.0134	482.1479	0.0734	966.3623	10.1398	1499.3215	7.3228
59.7929	0.3965	483.016	0.4663	966.7785	10.4861	1501.9449	6.629
78.491	1.4342	541.2321	0.2644	1048.9553	3.3337	1607.2729	14.1997
89.0883	0.0858	541.4728	3.0752	1050.6176	4.1689	1608.0475	147.0028
101.2143	7.358	548.9486	0.5345	1052.5814	2.3397	1620.5898	76.0466
103.5822	5.1626	549.1266	5.0519	1056.3804	1.6056	1624.0647	230.3202
123.1052	6.1392	661.4668	18.0395	1094.1389	39.3235	1633.2048	22.9768
127.3796	3.0096	662.5497	2.1107	1094.3667	64.4747	1634.0034	18.3162
150.451	3.4095	668.0229	0.449	1184.6285	15.6223	1664.0026	50.159
153.1326	1.5344	668.7801	0.2078	1184.7833	4.4717	1667.4041	334.8076
179.5611	0.7559	717.8515	14.8535	1208.917	6.8039	1668.4406	210.3268
185.8249	1.666	718.1848	26.9107	1209.2321	26.3875	1669.2795	166.2294
189.4679	0.2125	739.2918	111.0234	1220.4561	0.3392	3074.9392	0.8768
193.7987	7.0708	740.0657	7.4066	1222.2325	0.3771	3075.6946	0.259
194.5187	1.3655	760.1704	33.4574	1354.3826	15.2785	3146.9888	2.6818
199.9836	2.5218	760.7635	22.866	1355.7351	7.5663	3147.3743	4.1554
296.0558	3.3548	790.55	0.2145	1388.4705	610.8024	3180.3569	1.1336
296.6949	0.8447	791.5138	0.1071	1389.1523	31.4292	3180.9182	3.7902
324.7901	0.2067	796.5846	2.8469	1392.7549	647.5478	3255.7366	23.6929
325.6773	0.2503	796.7956	10.0258	1394.4088	58.375	3257.2678	21.2765
326.5354	0.035	805.9091	21.8258	1402.6722	1.3532	3258.4272	17.8489
329.1659	0.2011	806.2351	2.4385	1405.172	40.3744	3260.5779	14.6354

Table 16. Oscillation frequencies and IR intensities for 4-molecule cluster of TNT.

Frequency cm^{-1}	Intensity (km/mol)	Frequency cm^{-1}	Intensity (km/mol)	Frequency cm^{-1}	Intensity (km/mol)	Frequency cm^{-1}	Intensity (km/mol)
6.0037	0.0276	190.2879	0.3889	659.3755	11.1961	962.0534	9.2311
6.8127	0.0135	192.0548	3.329	659.8872	3.4303	962.7248	8.0756
9.5511	0.0445	192.7032	0.5122	661.2794	13.0666	963.062	0.6791
10.7137	0.0363	196.8943	5.2073	662.7278	9.7932	966.6378	8.1237
13.1434	0.1926	198.2761	5.0334	667.572	0.5246	968.2356	9.3892
14.6485	0.0858	199.7631	0.4605	669.3944	0.0793	1043.2646	8.177
17.4745	0.0361	202.1056	5.8742	672.8601	4.6511	1044.2894	6.1182
19.1606	0.0969	294.9276	1.4559	673.2171	2.6274	1048.3198	5.3386
21.5413	0.0717	296.7783	1.0261	716.6365	24.5244	1050.1333	2.0496
25.5663	0.2335	297.8845	2.4338	716.9527	13.5797	1050.6147	3.5367
27.2907	0.0672	298.8831	4.4941	718.0088	22.1708	1050.6708	3.3637
28.3122	0.0329	324.7092	0.2389	719.3519	18.0592	1052.1492	5.8976
32.3861	0.1016	325.209	0.6029	739.063	24.7206	1052.735	4.1214
34.9573	0.2077	325.7378	0.148	739.3708	130.8296	1096.455	75.916
40.7299	0.3467	325.811	0.0405	739.7837	7.1419	1096.6624	54.0083
45.9148	0.5988	328.6621	0.7673	740.7033	70.2921	1097.9261	37.4622
50.9682	0.136	329.6841	0.4998	759.5333	23.6246	1100.058	41.0888
51.3221	0.1839	330.0564	0.8057	759.7645	42.8882	1185.3416	7.8041
51.9382	0.6017	332.9135	0.1063	761.1715	20.4302	1185.6052	16.1508
52.3798	0.3453	353.4549	2.2863	761.3542	30.9627	1185.7306	10.7674
54.6865	0.0232	353.8611	2.0427	790.5221	0.8358	1186.6664	12.6373
55.5157	0.0207	354.4024	2.9248	790.5998	0.8792	1209.8322	15.0783
57.1434	0.358	355.4821	3.7328	791.1676	2.192	1212.8856	15.3057
62.0863	1.2134	366.9194	1.0839	791.3026	0.1507	1214.3346	13.1397
67.9725	0.2731	368.2383	1.9205	795.9496	5.5813	1217.5505	16.2261
73.8181	1.3738	369.3088	3.9455	796.7322	4.9704	1219.2219	0.5039
82.7084	0.6903	371.3992	4.807	797.4355	0.6989	1222.7281	10.706
91.401	0.4921	384.9266	1.092	797.6327	9.7116	1222.955	1.1508
95.9635	1.9103	385.0972	1.1167	805.0269	12.7807	1223.564	1.0288
99.4256	0.6227	388.1738	0.4284	805.3314	9.2942	1351.2896	9.5548
102.8424	1.2621	391.668	1.9364	806.0565	12.7468	1353.3455	4.2628
103.8391	9.4549	463.06	0.3618	807.2446	17.6478	1354.8254	5.0704
110.2973	5.5524	467.1603	1.1573	842.8611	0.756	1355.7509	6.9006
112.2823	14.0066	471.2585	0.2994	843.3628	3.0391	1387.3927	504.0168
124.5235	5.1683	472.1674	1.6982	844.5015	1.8451	1388.4775	243.7943
130.0222	1.9675	481.0948	0.1812	845.4727	2.1841	1388.7524	87.4017
132.8818	2.7792	483.7679	0.597	921.0493	17.8875	1389.0958	447.19
135.3963	1.4377	484.3633	1.0706	922.0851	40.7448	1392.4327	798.6592
147.6898	2.1166	485.0125	0.3554	923.0247	45.2336	1393.287	243.6454
152.6375	5.3	540.766	2.8936	923.3955	28.3322	1394.8691	156.6218
153.1419	2.6393	541.2985	1.5216	951.4396	6.7371	1396.2841	238.8504
157.2293	1.2297	542.3571	0.716	951.9678	39.1078	1402.8853	40.1082
165.0722	0.1527	542.7461	2.9325	953.4363	32.0243	1405.0447	2.3998
175.0778	0.79	549.0063	3.0966	953.5462	24.8804	1405.257	35.9898
178.4232	1.1197	549.4428	5.5645	954.3428	34.9316	1408.3396	49.7168
184.5245	1.3816	550.4266	3.418	955.4679	4.9786	1419.1819	11.4361
188.0139	2.7537	551.0865	2.0792	960.9208	3.5001	1419.2982	4.5842

Table 16 (continued)

Frequency cm^{-1}	Intensity (km/mol)	Frequency cm^{-1}	Intensity (km/mol)	Frequency cm^{-1}	Intensity (km/mol)	Frequency cm^{-1}	Intensity (km/mol)
1420.2479	5.2822	1497.4508	11.3855	1659.2784	20.6782	3152.1172	3.5304
1420.9575	11.7015	1499.9305	5.7411	1660.0342	35.6986	3177.7893	3.8554
1424.3171	6.9025	1499.9749	6.4007	1663.2992	146.911	3182.9602	2.5709
1424.7	14.2952	1602.7976	89.5147	1664.3833	383.5529	3190.4402	3.017
1425.6173	3.7006	1604.576	75.0732	1666.8501	298.8433	3204.1228	1.4827
1426.0646	3.5978	1605.7961	16.9799	1668.7557	154.036	3231.541	99.6425
1473.5498	9.0424	1606.5385	136.8389	1669.1105	13.3956	3253.373	20.5025
1474.6635	12.8272	1614.0665	33.3701	1669.4171	381.2602	3255.3308	23.642
1475.9045	16.0343	1615.7209	24.6628	3073.4512	2.0504	3255.5933	23.5913
1476.1462	5.7658	1617.3809	316.2843	3075.5383	0.5901	3256.0857	22.1997
1476.3361	10.2827	1623.7596	58.5519	3076.5342	0.1196	3257.0527	24.6223
1477.5513	3.2443	1624.993	121.0073	3076.7654	0.9591	3258.084	18.7786
1477.8824	21.6264	1630.8451	12.1011	3143.1304	3.4185	3265.4907	18.7129
1478.4861	10.8031	1632.7219	102.004	3149.0393	8.8789		
1494.5078	2.0778	1634.2406	2.0151	3149.7698	4.0967		

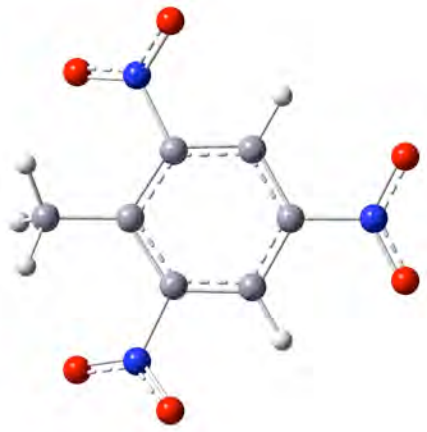

Figure 20. Molecular geometry of TNT

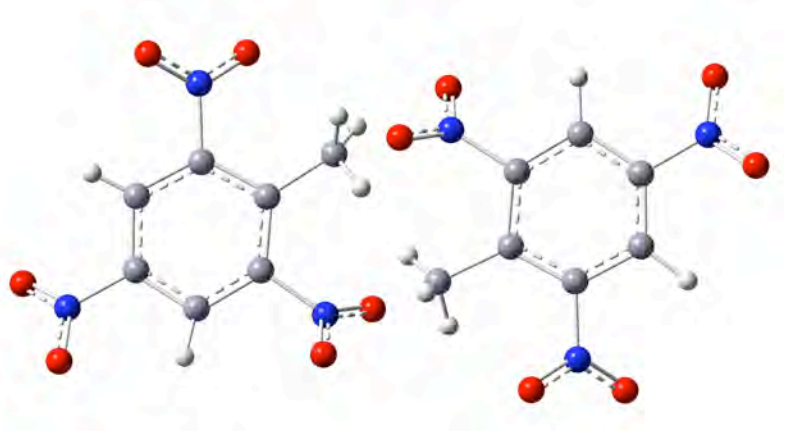

Figure 21. Molecular geometry of 2-molecule cluster of TNT

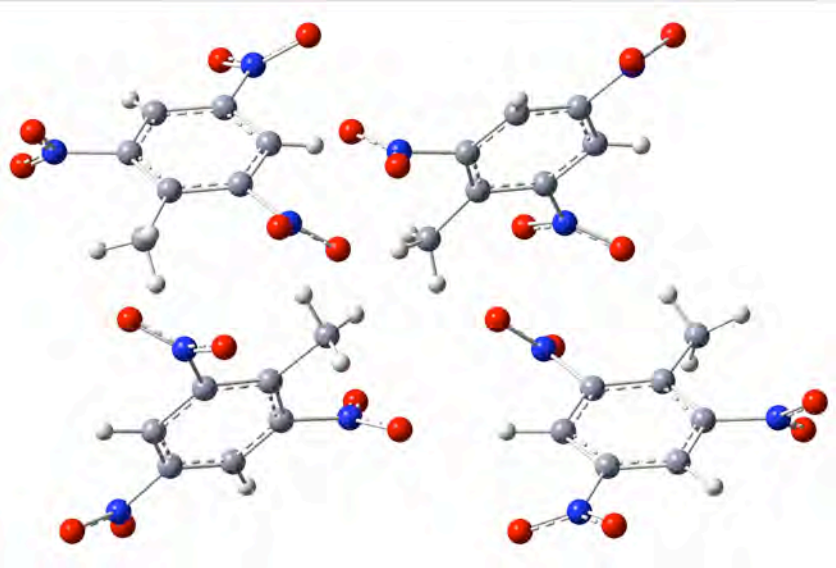

Figure 22. Molecular geometry of 4-molecule cluster of TNT

Proceeding, shown in Figs. 23, 24 and 25 are calculated IR intensities for a single isolated molecule and molecular clusters consisting of 2 and 4 molecules of TNT, respectively. Shown in Figs. 26, 27 and 28, are continuous spectra consisting of a superposition of essentially Lorenzian functions of various heights and widths, which have been constructed using the discrete spectra given in Tables 14, 15 and 16, respectively.

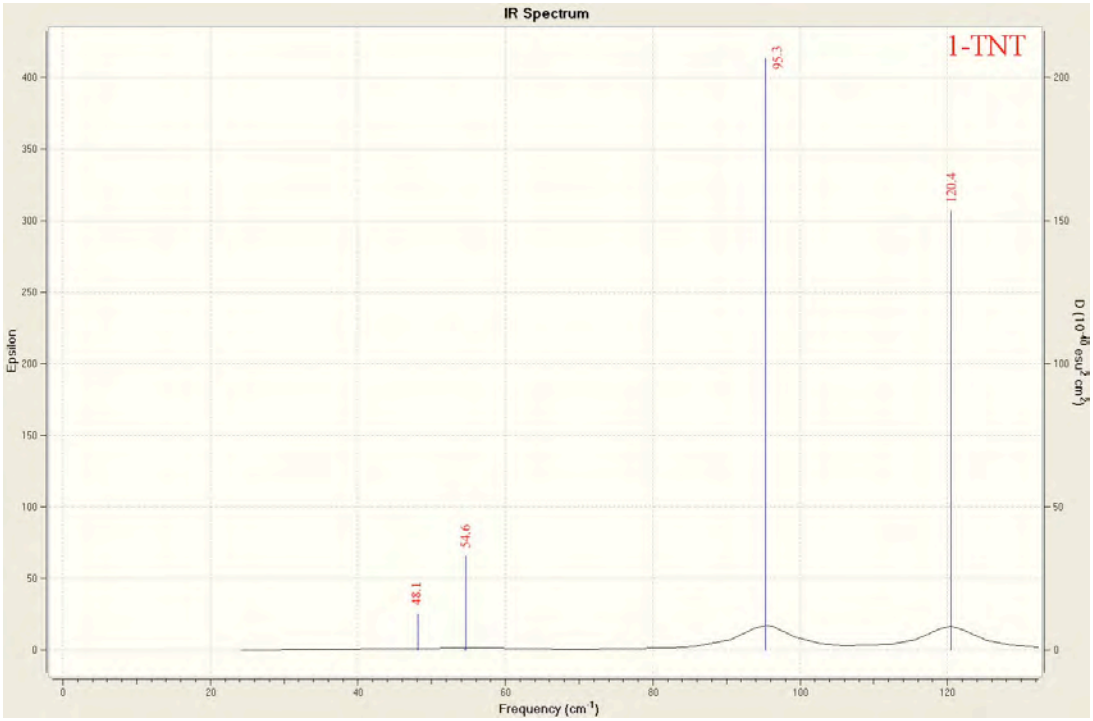

Figure 23. IR intensity as a function of frequency calculated using DFT B3LYP/6-311G(2d,2p) for single isolated molecule of TNT according to frozen phonon approximation.

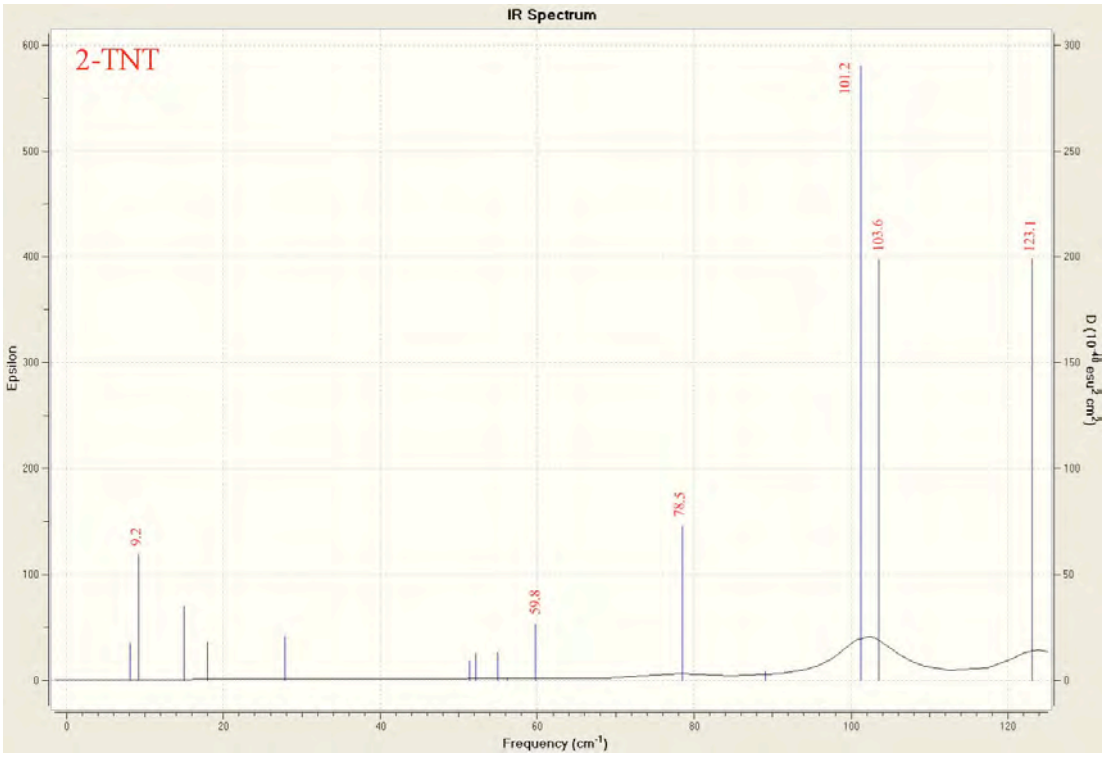

Figure 24. IR intensity as a function of frequency calculated using DFT B3LYP/6-311G(2d,2p) for two-molecule cluster of TNT according to frozen phonon approximation.

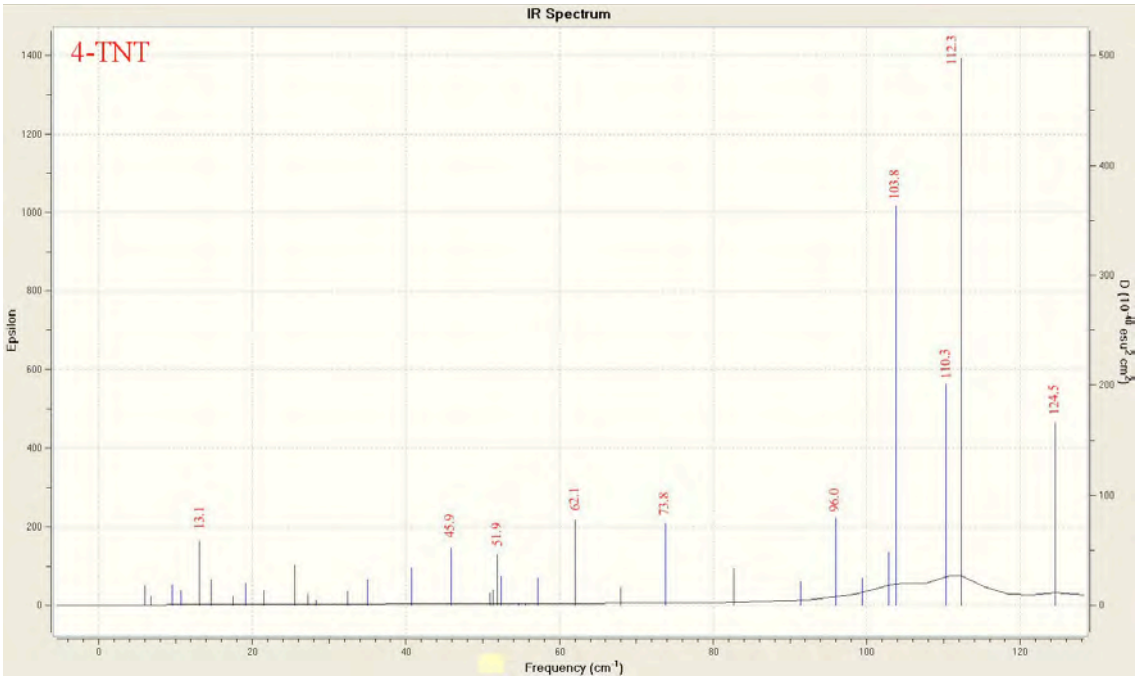

Figure 25. IR intensity as a function of frequency calculated using DFT B3LYP/6-311G(2d,2p) for four-molecule cluster of TNT according to frozen phonon approximation.

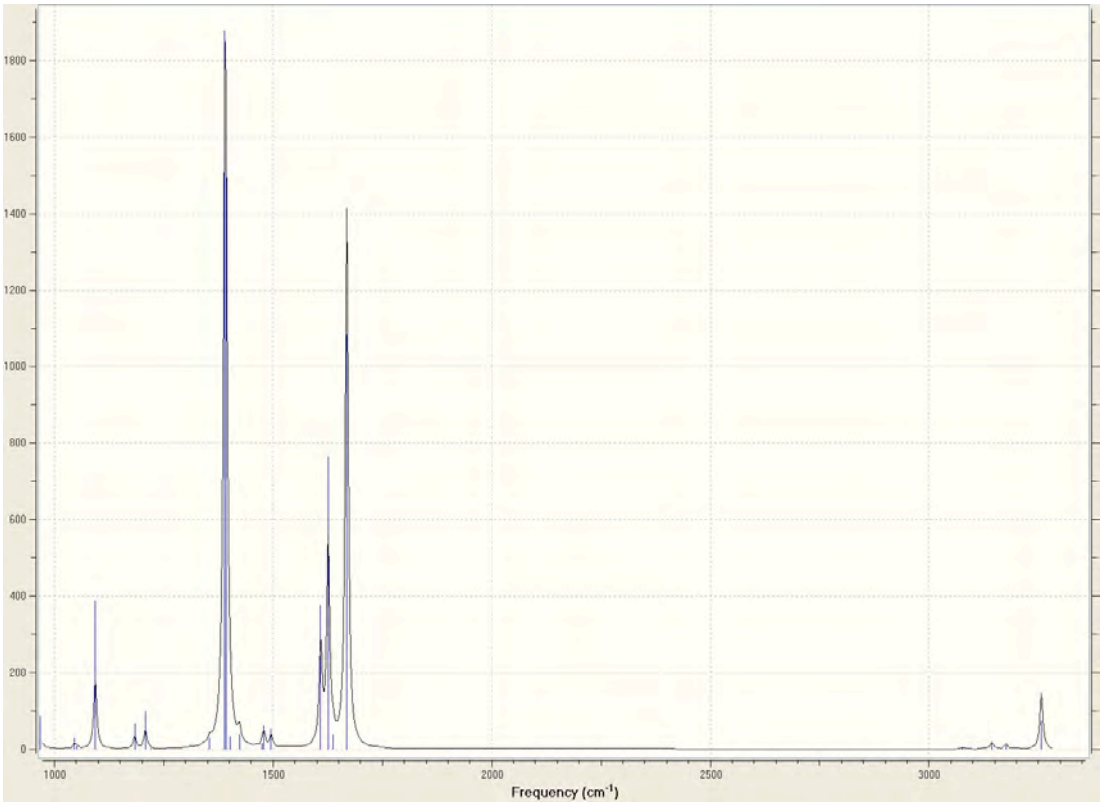

Figure 26. Continuous-spectrum representation of IR intensity as a function of frequency calculated using DFT for single isolated molecule of TNT.

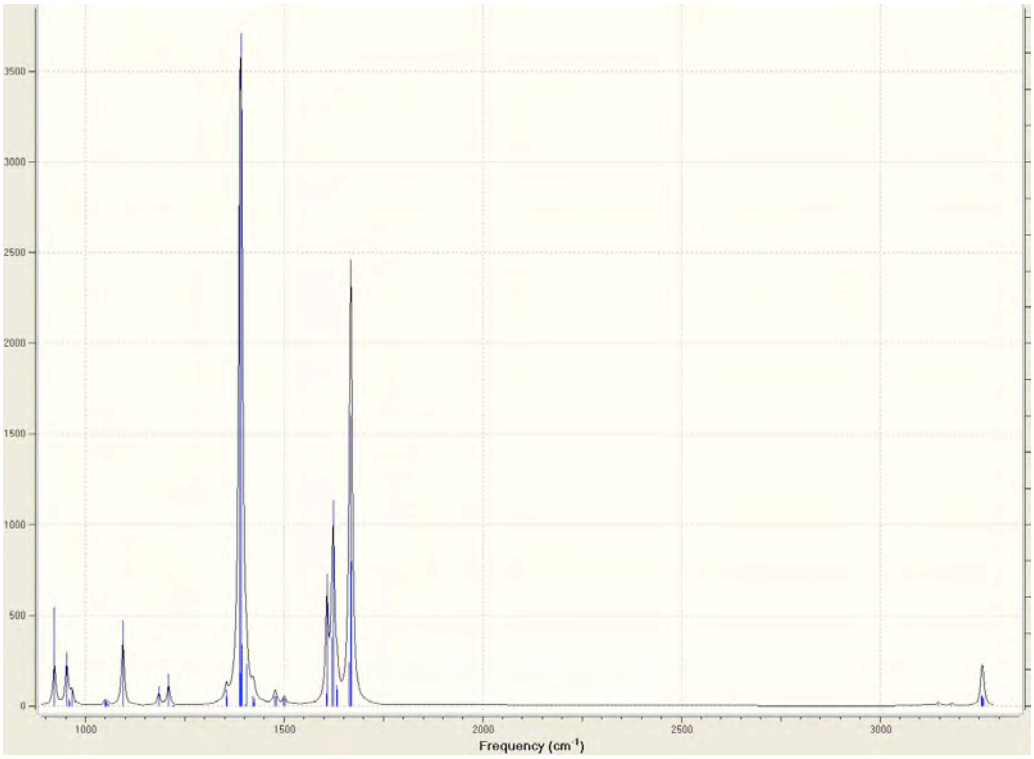

Figure 27. Continuous-spectrum representation of IR intensity as a function of frequency calculated using DFT for two-molecule cluster of TNT.

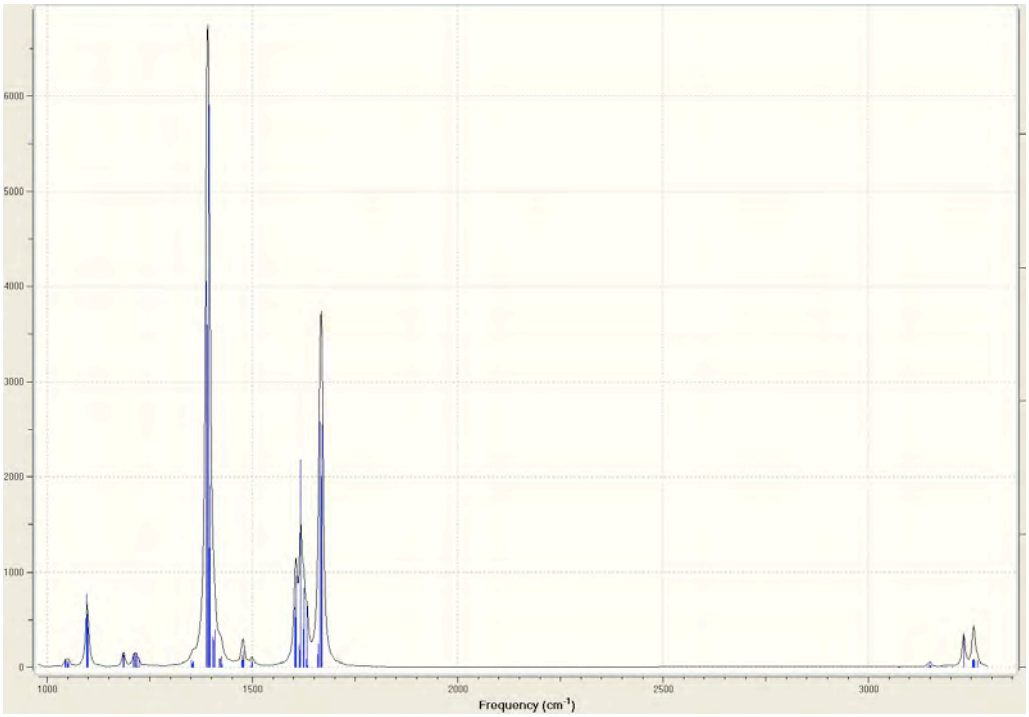

Figure 28. Continuous-spectrum representation of IR intensity as a function of frequency calculated using DFT for two-molecule cluster of TNT.

Shown in Figs. 29 and 30 are spectra of clusters in comparison with experimentally measured spectra [19, 20]. Referring to these figures, initial consideration is given to what extent various average features of the DFT calculated spectra for different size molecular clusters, as well as experimentally measured spectra, are correlated with each other. Referring to Fig. 29, one observes on average a noticeable correlation between DFT calculated spectra for molecule clusters of TNT and experimentally measured spectrum for dielectric response of TNT solid. The comparison of spectra shown in Fig. 29 also supports the notion that certain resonance features, which are associated with finite-size molecular clusters, are preserved within clusters of increasing size, as well as in solid form, thus implying a persistence of these modes after coupling to intermolecular influences. The persistence of certain intramolecular modes, which is irrespective of molecular cluster size, i.e., whether the molecule is isolated, part of a cluster or within a bulk lattice, is demonstrated by comparison of DFT calculated and experimentally measured spectra. Shown in Table 17 is a comparison of DFT calculated frequencies corresponding to prominent absorptions, which have been observed experimentally for TNT in solid state. Referring to this table, one can observe a high correlation between DFT calculated spectra for different cluster sizes and experimentally determined absorption lines at the specific frequencies indicated.

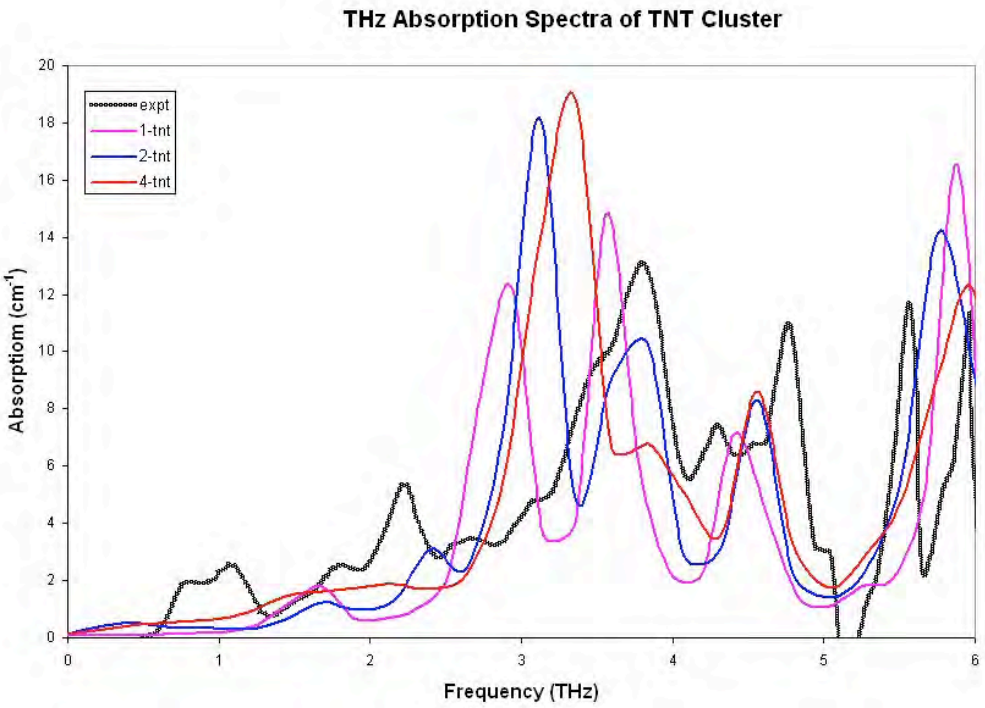

Figure 29. Qualitative comparison of DFT calculated spectra for 1-and 3-molecule clusters of TNT and experimentally measured spectrum for dielectric response of TNT solid.

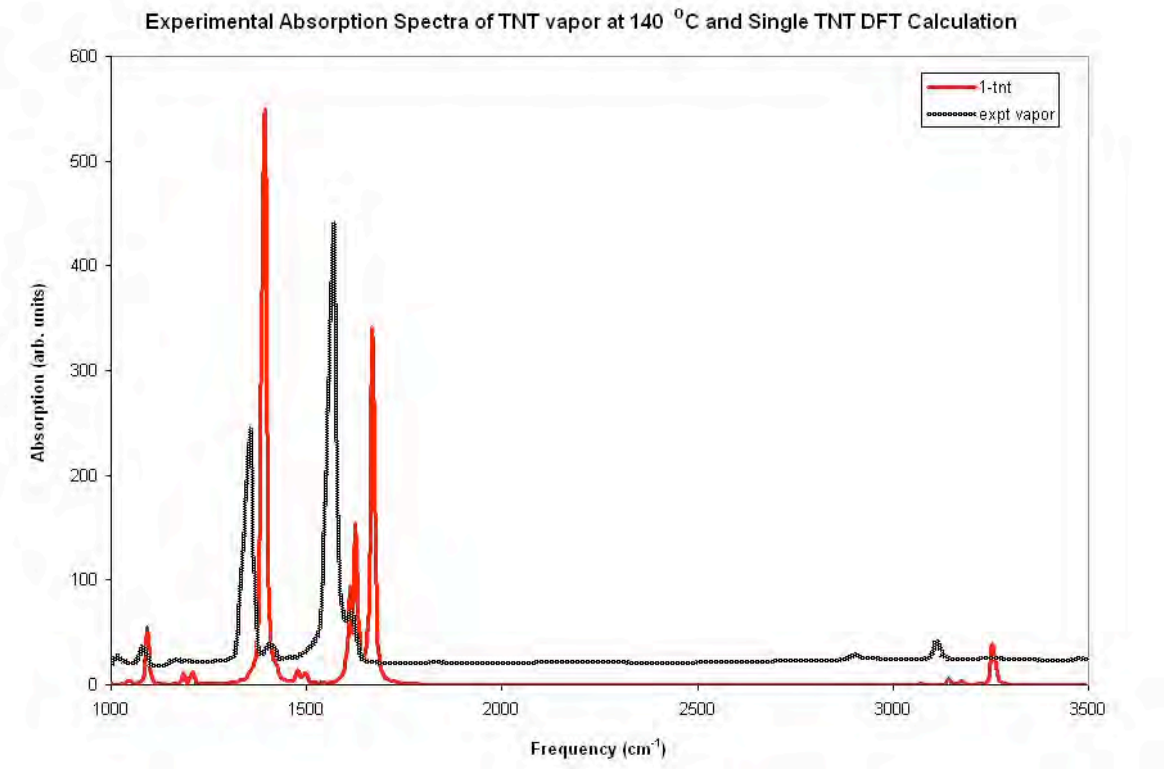

Figure 30(a). Qualitative comparison of DFT calculated spectra for single TNT and experimentally measured spectrum for dielectric response of TNT vapor.

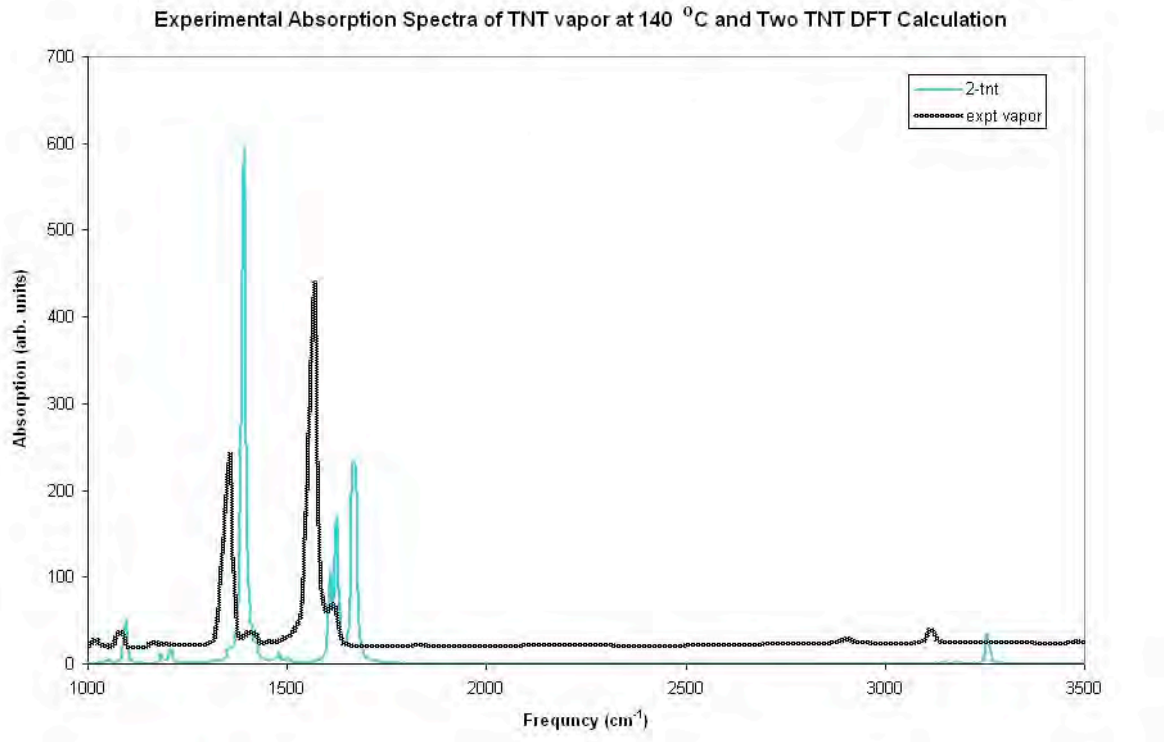

Figure 30(b). Qualitative comparison of DFT calculated spectra for 2-molecule clusters of TNT and experimentally measured spectrum for dielectric response of TNT vapor.

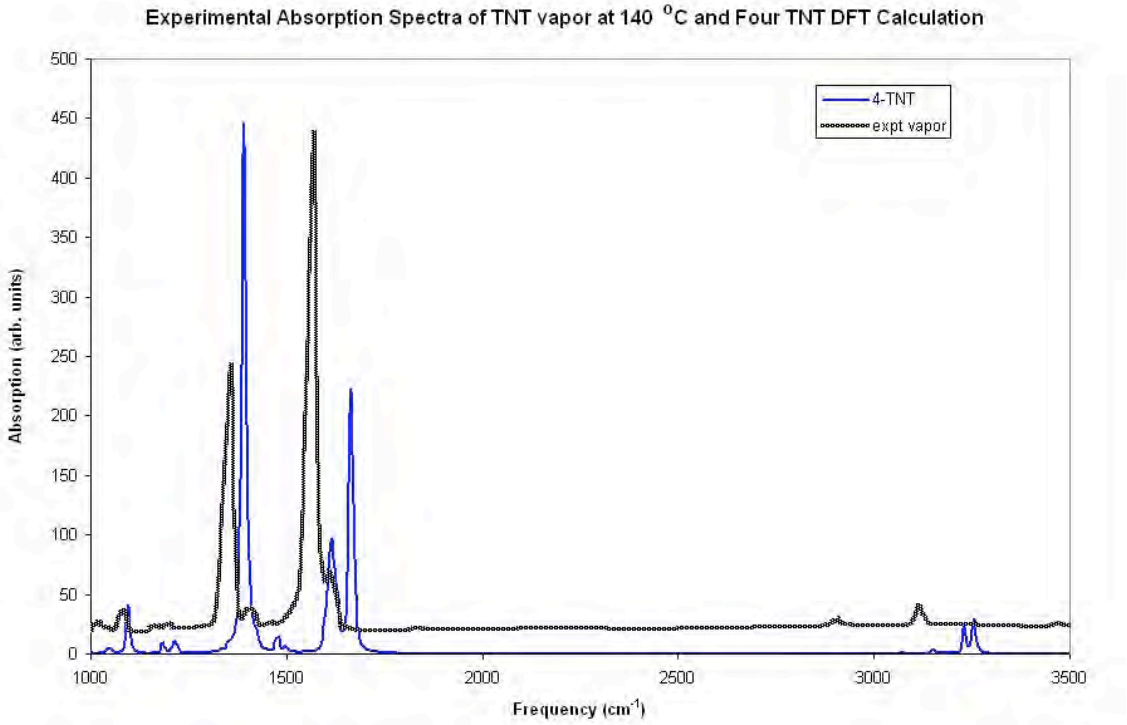

Figure 30(c). Qualitative comparison of DFT calculated spectra for 4-molecule clusters of TNT and experimentally measured spectrum for dielectric response of TNT vapor.

Table 17. Comparison of DFT calculated and experimentally measured frequencies at prominent absorptions for TNT solid [19].

Expt(cm^{-1})	53	73		127
1-TNT	48-55	(95)		120
2-TNT	60	79	(101-103)	123
4-TNT	52	74	(104-112)	125

Referring to Fig. 30, one observes on average a noticeable correlation between DFT calculated spectra for molecule clusters of TNT and experimentally measured spectrum for dielectric response of TNT vapor. Shown in Table 18 is a comparison of DFT calculated frequencies corresponding to prominent absorptions, which have been observed experimentally for TNT in vapor state. Referring to this table, one can observe a high correlation between DFT calculated spectra for different cluster sizes and experimentally determined absorption lines at the specific frequencies indicated.

Table 18. Comparison of DFT calculated and experimentally measured frequencies at prominent absorptions for TNT vapor [20].

Expt(cm^{-1})	1080	1349	1402	1559	1606	2898	3107
Paper calc.		1651 1654		1880 1883		3244 3324 3348	3440 3441
1-TNT	1093	1389	1392	1479-95	1608-68	3143	3257
2-TNT*	1094	1388	1393	1480-99	1608-67	3146	3255
4-TNT*	1096	1387	1392	1477	1617-69	3149	3231

Conclusion

The calculations of ground state resonance structure associated with molecular clusters of RDX, PETN and TNT using DFT are meant to serve as reasonable estimates of molecular level response characteristics, providing interpretation of dielectric response features, for subsequent adjustment relative to experimental measurements and molecular structure theory.

Acknowledgement

This work was supported by the Office of Naval Research.

References

[1] M. J. Frisch, G. W. Trucks, H. B. Schlegel, G. E. Scuseria, M. A. Robb, J. R. Cheeseman, G. Scalmani, V. Barone, B. Mennucci, G. A. Petersson, H. Nakatsuji, M. Caricato, X. Li, H. P. Hratchian, A. F. Izmaylov, J. Bloino, G. Zheng, J. L. Sonnenberg, M. Hada, M. Ehara, K. Toyota, R. Fukuda, J. Hasegawa, M. Ishida, T. Nakajima, Y. Honda, O. Kitao, H. Nakai, T. Vreven, J. A. Montgomery, Jr., J. E. Peralta, F. Ogliaro, M. Bearpark, J. J. Heyd, E. Brothers, K. N. Kudin, V. N. Staroverov, R. Kobayashi, J. Normand, K. Raghavachari, A. Rendell, J. C. Burant, S. S. Iyengar, J. Tomasi, M. Cossi, N. Rega, J. M. Millam, M. Klene, J. E. Knox, J. B. Cross, V. Bakken, C. Adamo, J. Jaramillo, R. Gomperts, R. E. Stratmann, O. Yazyev, A. J. Austin, R. Cammi, C. Pomelli, J. W. Ochterski, R. L. Martin, K. Morokuma, V. G. Zakrzewski, G. A. Voth, P. Salvador, J. J. Dannenberg, S. Dapprich, A. D. Daniels, Ö. Farkas, J. B. Foresman, J. V. Ortiz, J. Cioslowski, and D. J. Fox, Gaussian 09, Revision A.1, Gaussian, Inc., Wallingford CT, 2009.

[2] A. Frisch, M. J. Frisch, F. R. Clemente and G. W. Trucks, Gaussian 09 User's Reference, pp105-106 (2009)

[3] P. Hohenberg and W. Kohn, "Inhomogeneous Electron Gas" Phys. Rev. **136**, B864, (1964).

[4] W. Kohn and L. J. Sham, "Self-Consistent Equations Including Exchange and Correlation Effects" Phys. Rev. **140**, A1133 (1965).

[5] R.O. Jones and O. Gunnarson, "The density functional formalism, its applications and prospects" Rev. Mod. Phys. **61**, 689 (1989).

[6] W.W. Hager and H. Zhang, "A survey of nonlinear conjugate gradient methods," Pacific J. Optim., 2, p. 35-58 (2006).

[7] R. M. Martin, *Electronic Structures Basic Theory and Practical Methods*, Cambridge University Press, Cambridge 2004, p. 25.

[8] E. B. Wilson, J. C. Decius and P. C. Cross, *Molecular Vibrations* (McGraw-Hill, New York, 1955).

[9] J.W. Ochterski, "Vibrational Analysis in Gaussian," help@gaussian.com, 1999.

[10] C. A. D. Roeser and E. Mazur, "Light-Matter Interactions on Femtosecond Time Scale" in *Frontiers of Optical Spectroscopy*, eds. B. Di Bartolo and O. Forte, NATO Science Series v. 168 p. 29, Kluwer Academic Publishers, Dordrecht – Norwell, 2005; C. F. Bohren and D. R. Huffman, *Absorption and Scattering of Light by Small Particles* (Wiley-VCH Verlag, Weinheim, 2004).

[11] A. Shabaev, S. G. Lambrakos, N. Bernstein, V. L. Jacobs, D. Finkenstadt, "A General Framework for Numerical Simulation of IED-Detection Scenarios using Density Functional Theory and THz Spectra," Applied Spectroscopy, **65**, 409-416 (2011).

[12] A. D. Becke, "Density-functional Thermochemistry. III. The Role of Exact Exchange", *J. Chem. Phys.* **98**, 5648-5652 (1993).

[13] B. Miehlich, A. Savin, H. Stoll and H. Preuss, "Results of Obtained with the Correlation Energy Density Functionals of Becke and Lee, Yang and Parr", Chem. *Phys. Lett.* **157**, 200-206 (1989).

[14] A. D. McLean and G. S. Chandler, "Contracted Gaussian-basis sets for molecular calculations. 1. 2nd row atoms, Z=11-18," *J. Chem. Phys.*, **72** 5639-48 (1980).

[15] T. Clark, J. Chandrasekhar, G. W. Spitznagel and P. V. R. Schleyer, "Efficient diffuse function-augmented basis-sets for anion calculations. 3. The 3-21+G basis set for 1st-row elements, Li-F," *J. Comp. Chem.*, **4** 294-301, (1983).

[16] M. J. Frisch, J. A. Pople and J. S. Binkley, "Self-Consistent Molecular Orbital Methods. 25. Supplementary Functions for Gaussian Basis Sets," *J. Chem. Phys.*, **80** (1984) 3265-69.

[17] C.S. Choi and E. Prince, *Acta Crystallogr., Sect.B:Struct. Crystallogr.Cryst.Chem.* **28,** 2857-2862.

[18] I. J. Bruno, J. C. Cole, P. R. Edgington, M. K. Kessler, C. F. Macrae, P.McCabe, J. Pearson and R. Taylor, *"New software for seaching the Cambridge Structural Database and visualizing crystal structures"*, Acta Cryst. (2002) B58, 389-397.

[19] T. Lo, I.S. Gregory, C. Baker, P.F. Taday, W.R. Tribe and M.C. Kemp, "The very far-infrared spectra of energetic materials and possible confusion materials using terahertz pulsed spectroscopy" *Vibrational Spectroscopy* 42 (2006) pp243-248.

[20] J. Janni, B.D. Gilbert, R.W. Field, and J.I. Steinfeld, "Infrared aborption of explosive molecule vapors" *Spectrochimica Acta* pat A 53 (1997) pp1375-1381.